10 Leak growth mechanism in composite Pd membranes

10.1 Introduction

Membranes Ma-32b/34b/42 showed that the selectivity (H_2/He) decreased as a function of time when the membrane was held at 500ºC in H_2 atmosphere (see Section 0 and Table 6-2). Thermal and hydrogen stresses were found to play a small role in leak formation since holding a composite Pd membrane at low temperatures, when compressive stresses were the highest, did not lead to leak formation. Indeed, all membranes showed high (>1000) H_2 permselectivities at temperatures lower than 400ºC (see Figure 6-10). However, it was very interesting to note that thermal stress release started to occur at 400ºC when the energy barrier for diffusion was overcome and that selectivity started to decrease at temperatures close to 400-450ºC (see Figure 6-10).

The main objective of this part of the thesis was to investigate the process taking place at temperatures close to 400-450ºC that led to leak growth. The shape and size of defects were also studied. Also, the leak distribution on the surface was examined to determine whether leakage in composite Pd membranes was a localized phenomenon or a process taking place over the entire surface of the membrane. In addition, the rate at which the He leak of composite Pd membranes increased as a function of time was measured at different temperatures to estimate the activation energy of the rate of increase of the leak. The

order of magnitude of the activation energy would provide information on the mechanism underlying the leak formation and leak growth.

10.2 Experimental

10.2.1 Membrane preparation

The composite Pd membranes studied in this chapter are listed in Table 10-1. C01-F11/11b membranes were prepared on graded PSS supports and Ma-32b/34b/41/42 membranes were prepared on graded PH supports. All membranes were prepared according to the experimental procedure described in Chapter 3. Composite Pd membranes were characterized in the set-up described in Section 3.2.1.

10.2.2 Membrane characterization procedures

The characterization of membranes C01-F11a/b was described in detailed in Section 5.4.4.

Membrane Ma-32b was heated up to 500ºC in He atmosphere at a rate of 0.5ºC/min and then H_2 was introduced. The membrane was kept in H_2 atmosphere (ΔP=1 bar) at 500ºC for a period of 1,100 hr. The He leak of the membrane was measured frequently by switching from H_2 to He atmosphere at a constant pressure difference of 1 bar.

The characterization procedure of membrane Ma-34b needs to be described in detail since it deviated considerably from the characterization procedure described in Sections 3.2.2 and 3.2.3. Membrane Ma-34b was first characterized in H_2 atmosphere at 250, 300, 350 and 400ºC. It was then removed from the characterization set-up and stored at atmospheric conditions for more than a month. The membrane was characterized for a second time at 400, 450, 500, 550 and 600ºC. The H_2 permeance at 400ºC before and af-

ter storage at atmospheric conditions was the same indicating that the membrane did not deteriorate during storage. After checking that the H_2 permeance and the He leak at 400ºC were the same before and after storage, Ma-34b was heated to 450ºC. At 450ºC, membrane Ma-34b was held in He atmosphere and the He leak was monitored for 200 hr. H_2 was then introduced at 450ºC and the H_2 permeance monitored for 500 hr.

Table 10-1 Characteristics of composite Pd membranes considered in this chapter

Membrane	Support type	Grade (μm)	Ox. Temp	Thickness (μm)	Permeance at 500ºC	Final selectivity (H_2/He)
C01-F11	PSS	0.1	500	17	21	683
C01-F11b	C01-F11	0.1	500	19	23.5	478
Ma-32b	PH	0.1 medium	700	10	42	280
Ma-34b	Ma-34	0.1 coarse	700	8	24 (450ºC)	86
Ma-41	PH	0.1 coarse	700	10	30 (450ºC)	857
Ma-42	PH	0.1 medium	700	5.6	38.8	818

During the 500 hr-period the membrane was in H_2 atmosphere, the He leak was determined by switching from a pure H_2 feed to a feed containing 99%H_2-1%He. The composition of the permeate was analyzed by a on-line GC to obtain the ideal separation factor, or selectivity, (H_2/He). After 500 hr in H_2, the He leak of Ma-34b was measured in He atmosphere in order to determine if the He measurements with the GC were in agreement with the He leak measurements performed in He atmosphere as described in Section 3.3.1. The temperature was then raised up to 500ºC. The membrane was held at 500ºC in He atmosphere for 1500 hr and the He leak was measured regularly as described in Section 3.3.1. After 1500 hr in He atmosphere, H_2 was introduced at 500ºC and the H_2 permeance and leak were monitored for an additional 500 hr. At 500ºC, leaks were measured by switching from H_2 to He atmosphere. The remaining steps of the characterization

of membrane Ma-34b consisted of holding for 100 hr in H_2 atmosphere at 550 and 600ºC. At each temperature, the He leak was measured 3 or 4 times by switching from H_2 to He.

Membrane Ma-41, a composite Pd-Cu membrane, was characterized at 250, 300, 350 and 400ºC according to the procedure described in Sections 3.2.2 and 3.2.3. At 450ºC Ma-41 was held for 500 hr in H_2 atmosphere; the leak was determined by switching from pure H_2 to a 99%H_2-1%He mixture and measuring the permeate gas composition with an on-line GC. After 500 hr at 450ºC, He was introduced and the leak was measured in He atmosphere to corroborate the GC leak measurements previously taken. The temperature was then raised to 500ºC and H_2 was introduced. Ma-41 was not held at 500ºC in He atmosphere as was the case for Ma-34b. Ma-41 was held for 280 hr in H_2 atmosphere and the He leak was measured 3 or 4 times by switching from H_2 to He. Finally membrane Ma-42, was characterized as described in Sections 3.2.2 and 3.2.3

10.2.3 The activation energy for the rate of increase of leaks in composite Pd membranes

At a given temperature, leaks in composite Pd membranes were assumed to increase linearly with time, which turned out to be a good approximation at temperatures equal to or higher than 450ºC. The behavior of leaks at temperatures lower than 450ºC was difficult to study since they grew at a very slow rate. At temperatures higher than 450ºC, the leak was measured several times at a given temperature. Therefore, the rate at which the leak increased was determined relatively accurately. Yet, in cases, especially at low temperatures, only one leak measurement was performed. When only one leak measurement was available the rate at which the leak increased was calculated using the following procedure.

Figure 10-1 depicts the H_2 permeance as a function of time for an hypothetical membrane. At *t1* He was introduced and the He leak at 450ºC was measured. At *t2* the temperature was changed from 450ºC to 500ºC at a rate of 1ºC/min and *t3* was the time at which the He leak at 500ºC was measured.

Based on experimental observations, the He leak did not change during the 50 minutes that were necessary to bring the temperature up by 50ºC (e.g. from 450 to 500ºC). Therefore, the He leak at point *t2* was equal to the He leak at point *t1* plus the increase in He leak that occurred at 450ºC during the time $\Delta t = t2 - t1$. The rate of increase for the leak at 500ºC was then given by Equation (10-1)

$$rHe_{500} = \frac{He(t3) - \left\{He(t1) + rHe_{450} \cdot (t2 - t1)\right\}}{t3 - t2} \qquad (10\text{-}1)$$

where, $He(ti)$ is the He leak at the time ti (i=1, 2, 3, etc.) and rHe_{temp} is the rate of increase for the He leak at the temperature denoted in the subscript (*temp*). t_i corresponded to the time at which He leaks were measured and temperatures were changed as shown in Figure 10-1.

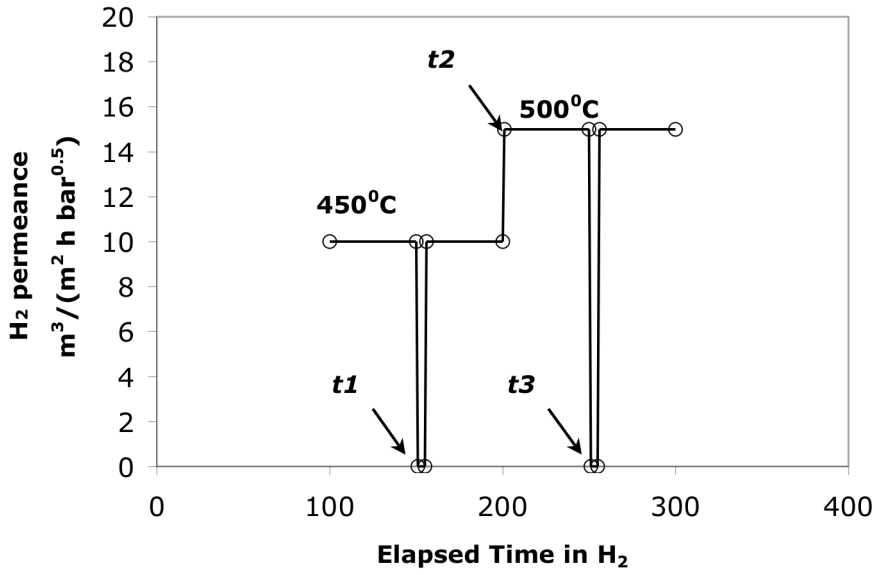

Figure 10-1 Schematic H_2 vs. time plot for a composite Pd membrane.

10.3 Results and discussion

10.3.1 Pinhole size, pinhole formation

10.3.1.1 Size characterization of pinholes

This section aimed at the study of defects already formed in a composite Pd membrane. The calculations are only shown for membrane Ma-41 at 450ºC although the same calculations were performed for all membranes.

The diffusion of gases through the defects in a Pd layer can be approximately given by the sum of a Knudsen term and a viscous term (slip-flow) as shown in Equation (10-2).

As already stated in Section 5.4.2, the flux of inert gases through defects was modeled as the flux of gases through a porous media with a very small porosity (Mardilovich et al., 1998). The flux of gases through defects was in general very small, therefore, leaks were not affected by mass transfer within the porous support. That is, when looking at Figure 5-1, the pressure P_2 is equal to pressure P_3.

$$\frac{J}{\Delta P} = \alpha + \beta \cdot P_{ave} = \frac{2}{6}\sqrt{\frac{8}{\pi}}\frac{\varepsilon \mu_k d}{L_{Pd}\sqrt{RTM}} + \frac{1}{32}\frac{\varepsilon \mu_v d^2}{L_{Pd}\eta RT}\cdot P_{ave} \qquad (10\text{-}2)$$

where $\alpha \cdot \Delta P$ is the Knudsen flow and $\beta \cdot \Delta P \cdot P_{ave}$ is the viscous flow. Equation (10-2) assumes that surface diffusion is negligible. Plotting gas permeance ($J/\Delta P$) as a function of the trans-membrane average pressure led to a straight line for every gas (He, N_2, Ar etc…) with α as the y-intercept and β as the slope. Figure 10-2 shows the permeance of He and Ar through Ma-41 as a function of the average trans-membranes pressure. Equation (10-2) also assumes that the defects of composite Pd membranes were pinholes within the Pd layer with an average diameter d. The average diameter d can be estimated from the β/α ratio after having assumed μ_k is equal to μ_v. After simplification, the β/α ratio is given by Equation (10-3)

$$\frac{\beta}{\alpha} = \theta \cdot \frac{3}{32}\cdot\sqrt{\frac{\pi}{8}}\cdot\frac{1}{\sqrt{RT}}\cdot\frac{\sqrt{M}}{\eta}d \qquad (10\text{-}3)$$

In fact μ_v is equal to $1/\tau$ and μ_k is equal $1/(\tau\ \theta_k)$ with θ_k the reflection factor. The reflection factor is proportional to the roughness of the pore walls. Smooth walls are characterized by a θ_k value equal to 1 while rough surfaces have reflection factors greater than 1. Therefore, assuming μ_k is equal to μ_v is equivalent to assume θ_k equal to 1 and that pinhole walls were smooth, which was close to the reality.

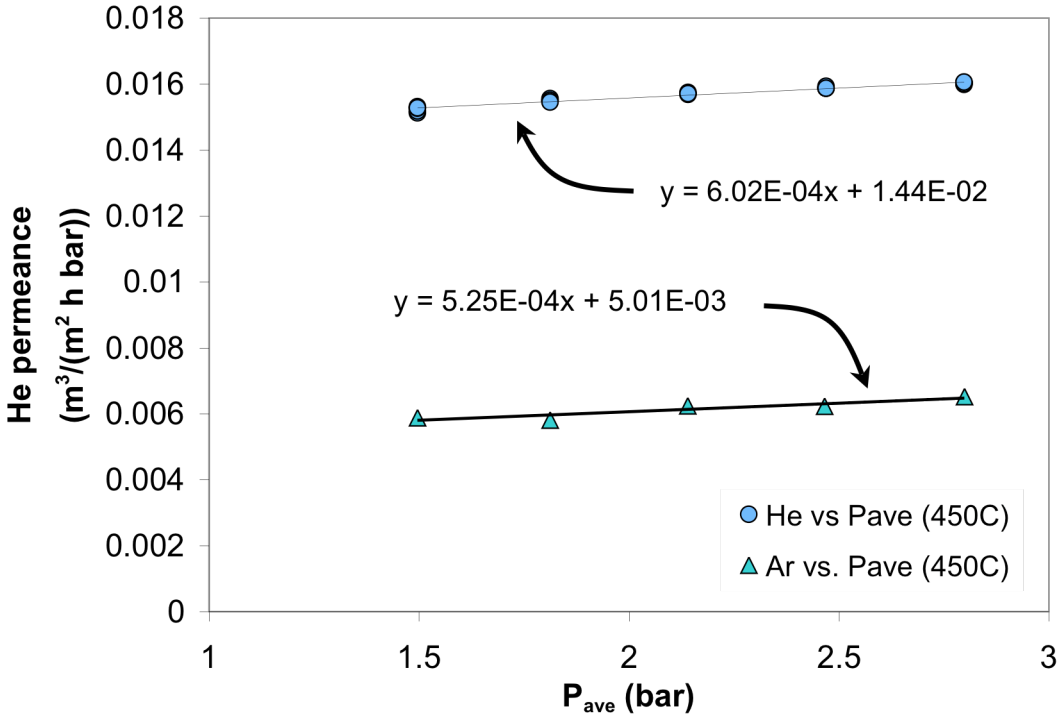

Figure 10-2 He and Ar permeance of Ma-41 as a function of average pressure across the membrane.

The β/α ratio of all gases can then be plotted as a function of $\sqrt{M}/\eta$ and be fitted with a straight line forced through the origin. Figure 10-3 shows the β/α ratio plotted as a function of $\sqrt{M}/\eta$ for He and Ar. The precision achieved on the determination of the diameter depended on the precision with which the β/α ratio was measured. The precision on the β/α ratio was estimated to be 1-2% when digital mass flow meters (MFM) were used. When bubble flow meters (BFM) were used for the measurement of the He permeance the precision on the β/α ratio dropped to 10-15%. He leak data from MFM were used when the He fluxes measured in the 0-4.5 bar (see Section 3.3.1) lay within the range of the mass flow meter (0-50sccm). The pinhole diameter was estimated with a 2-5% precision when data from MFM were used. The average pinhole size for Ma-41 was estimated to be 0.16 μm at 450ºC.

Table 10-2 summarizes the He leak and selectivity shown by all membranes after they were kept at the maximum temperature for the time listed in the Table. It became apparent that all composite Pd membranes suffered from selectivity reduction. Table 10-2 also lists the average pinhole size determined on each membrane. Membranes having a high selectivity (>800), Ma-41/42 were characterized by a very small average pinhole size equal to 0.16-0.17 μm. Membranes having a low selectivity (<100) were characterized by an average pinhole size larger than a micron.

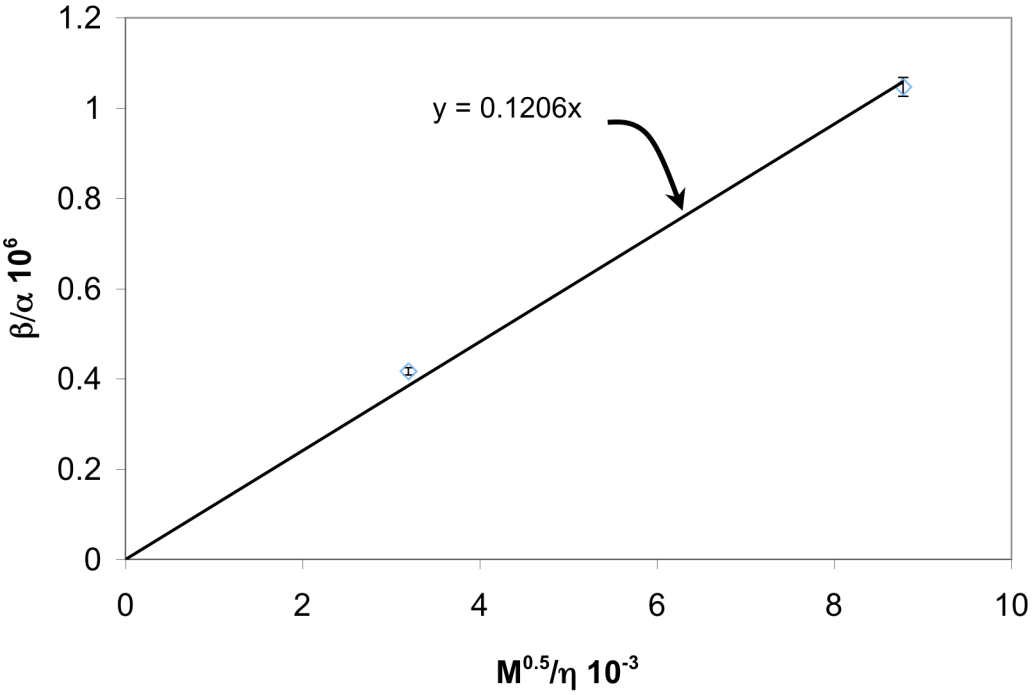

Figure 10-3 β/α ratio as a function of $M^{0.5}/\eta$ for He and Ar.

Table 10-2 He leak and selectivity of membranes considered in this chapter

membrane	Thick. (Weight gain) (μm)	Temp. (ºC)	Time spent at max Temp. (hr)	H_2 permeance at Temp. (col. 2) (m^3/m^2-h-$bar^{0.5}$)	He leak. (m^3/m^2-h-bar)	Selectivity at ΔP=1bar (H_2/He)	Average pinhole diameter (μm)
C01-F03	32	500	35	4.3	0.0148 (at RT) (BFM)	120	1.7 (at RT, He)
C01-F05	33	500	100	10.3	0.00766	587	n.d.
C01-F07	23	500	76	8	0.0763 (at RT) (BFM)	43	0.34 (at RT, He)
C01-F11	15	500	319	20.6	0.0125	683	0.83 (He)
C01-F11b	17	500	179	23.5	0.0214	478	0.47 (He)
C01-F11b	17	550	93	28.3	0.234 (at RT) (BFM)	52	0.34 (at RT, He and N_2)
Ma-32	7.7	500	52	50	0.485	42	n.d.
Ma-32b	10	500	1100	41	0.0651	280	n. d.
Ma-32c	12	500	556	38	1.101 (at RT) (BFM)	14	1.3 (at RT, He)
Ma-34b	8	500	552	20	0.0957	86	0.92 (He)
Ma-41	10	450	500	30	0.0145	857	0.16-0.17 (He and Ar)
Ma-42	5.6	500	111	39	0.0165	980	0.04 (He)
Ma-42	5.6	500	185	39	0.019	818	0.16 (He)

n.d. = not determined

10.3.1.2 The formation of pinholes at high temperatures

The morphology changes of Pd deposits formed by the electroless deposition method were studied by heating pieces of Ma-32c membrane at 500, 550, 600 and 650ºC for 48 hr in H_2 atmosphere. Figure 10-4(a), (b), (c) and (d) show the morphology of Ma-32c after the H_2 characterization at 500ºC, after the heat-treatment at 550, 600 and 650ºC respectively. No pinholes were readily seen on the surface of membrane Ma-32c after H_2 characterization at 500ºC. Figure 10-4(b) shows that the heat-treatment at 550ºC led to the growth of Pd clusters, yet pinholes were still not readily visible on a random region of the surface of the Pd layer. The heat-treatment at 600 and 650ºC led to the formation of a large number of pinholes, which were visible on random regions of Ma-32c surface. The number of pinholes per unit area was larger in the 650ºC annealed sample than in the 600ºC annealed sample.

Since high temperatures (600-650ºC) led to the formation of numerous and large (5μm in diameter) pinholes, and since few and small (1μm in diameter) pinholes were found at 500ºC, leak formation and growth might start at low temperatures 400-450ºC by the formation of small pinholes and leaks might grow at higher temperatures by the formation of new pinholes and growth of already formed pinholes. Section 10.3.1.3 aimed at the elucidation of the formation and growth of pinholes at moderate temperatures (450-550ºC).

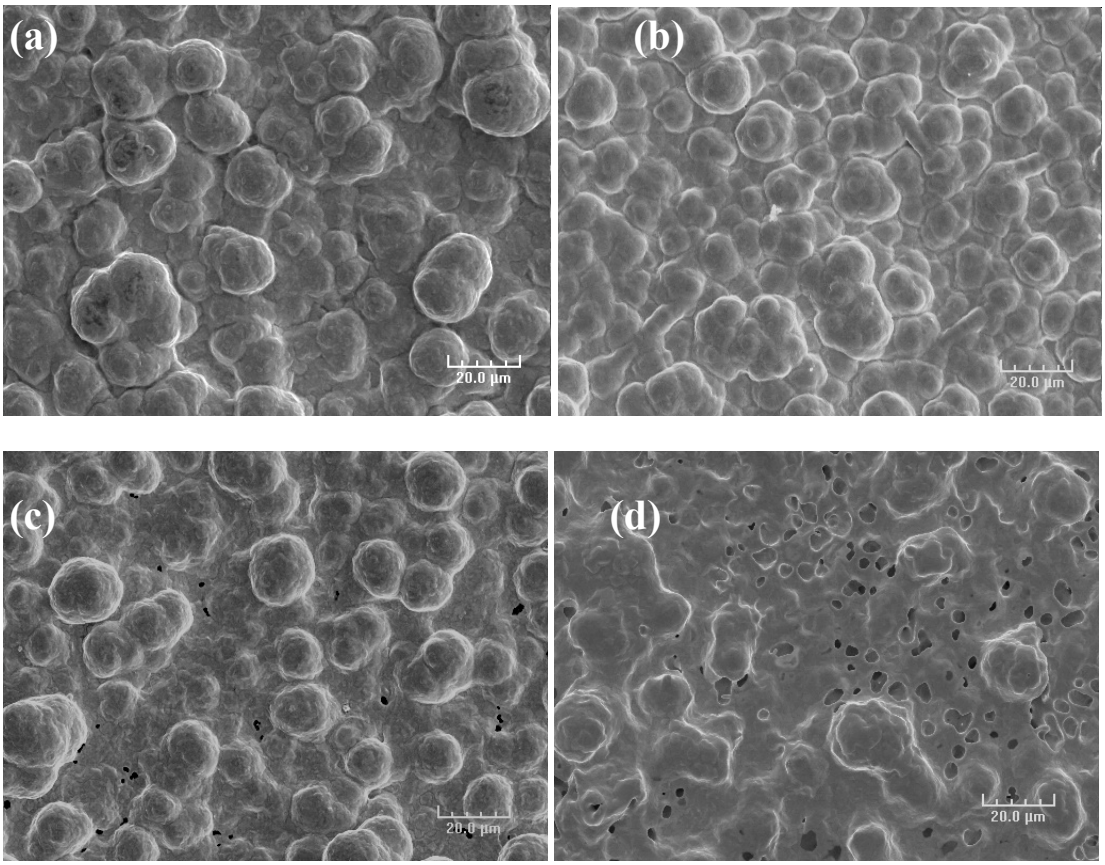

Figure 10-4 Ma-32c surface morphology after annealing in H_2 at (a) 500, (b) 550, (c) 600 and (d) 650ºC for 48 hr (Mag 1500)

10.3.1.3 The formation and growth of pinholes

This section aimed at the elucidation of the formation and growth of pinholes at the temperature at which leaks appeared in all composite Pd membranes, which was 450ºC (see Figure 6-10), and also at high temperatures (500 and 550ºC).

In order to investigate the formation and growth of pinholes at 450, 500 and 550ºC, the He permeance, the total pinhole surface, the pinhole diameter and the number of pinholes were determined as a function of time at 450 and 500ºC for membrane Ma-41 and at 500 and 550ºC for membrane Ma-34b. Figure 10-5 shows the He leak vs. average pressure at different times during the characterization of Ma-34b. In order to determine the He permeance, the total pinhole surface, the pinhole diameter and the number of pinholes were determined as a function of time, the He flux was measured at several pressures (see Section 3.2.3) and also at different times for a given temperature. As an example Figure 10-5 shows the raw data taken for membrane Ma-34b. The same type of data was also collected for Ma-41. The He permeance was measured after 1500 hr in He (circles in Figure 10-5), which was taken to be the zero time for the next H_2 characterization step. The He permeance of Ma-34b was also measured after 200, 400 and 550 hr after switching from H_2 to He atmosphere (Figure 10-5). The temperature was increased to 550ºC and the He permeance was measured after 60 hr. Figure 10-5 shows that for the first four lines (He permeance vs. P_{ave}) the ratio β/α increased, indicating an increase of the average pinhole diameter according to Equation (10-3) as the membrane was held at 500ºC in H_2. The straight line fitted through the experimental data taken at 550ºC clearly shows a lower β/α ratio indicative of a smaller average pinhole diameter at 550ºC.

The number of pinholes in the Pd layer can be estimated by first calculating the porosity ε of the Pd layer (Mardilovich et al., 1998) using Equation (10-4)b

$$\varepsilon_\beta = 8 \cdot L \cdot \eta \cdot \tau \cdot RT \cdot \beta \cdot \frac{4}{d^2} \qquad (10\text{-}4)a$$

$$\varepsilon_\alpha = \frac{3}{2}\sqrt{\frac{\pi}{8}} \cdot L \cdot \sqrt{RTM} \cdot \tau \cdot \alpha \cdot \frac{2}{d} \qquad (10\text{-}4)b$$

The tortuosity value τ was taken to be equal to 3.5, which is a general tortuosity value found in many pore systems.

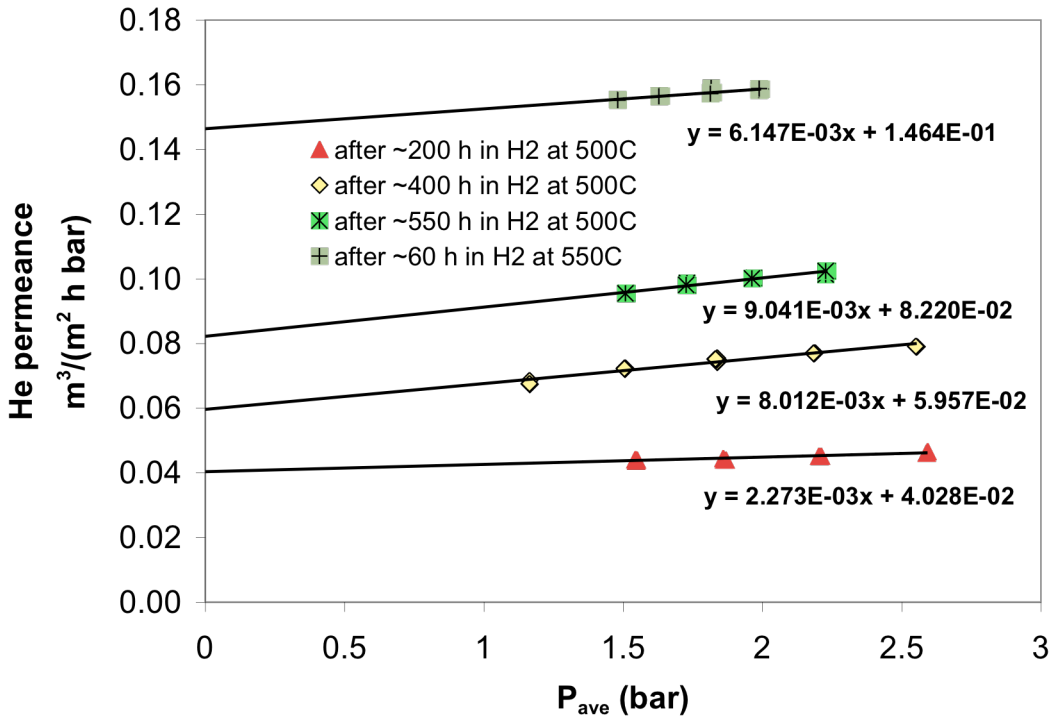

Figure 10-5 He permeance vs. average pressure at 500ºC at time t=0, 200, 400 and 550 hr and t=60 hr at 550ºC.

A greater precision was achieved using α than using β, which was due to somewhat larger errors on the determination of β. Therefore, porosity calculations based on α had a better precision. The number of pinholes per unit area can then be calculated from Equation (10-5)

$$N = 4 \cdot \frac{\varepsilon \cdot S}{\pi d^2} \qquad (10\text{-}5)$$

where N is the number of pinholes/m^2 and S the total surface of the composite Pd membrane. Since N is based on the porosity, a better estimation is found using ε based on α. ε·S is the total pinhole area.

Figure 10-6 shows the He permeance and the total pinhole area for membrane Ma-41 as a function of time at 450 and 500ºC. the total pinhole area (ε_α·S) as a function of time was calculated using experimental data similar to the one in Figure 10-5 and Equations (10-3) to (10-5). At 500ºC, both the leak rate and the total pinhole area increased linearly with time. Figure 10-7 shows the average pinhole diameter and the total number of pinholes in the 120 cm^2 of membrane Ma-41 as a function of time at 450ºC and 500ºC. The average pinhole diameter and the total number of the pinholes was also estimated using Equations (10-3), (10-4b) and (10-5). The average pinhole diameter decreased as a function of time from 0.42 to 0.25 μm at 500ºC. The number of pinholes slowly increased from around 1000 to around 6500. Therefore, it appeared that the He leak grew at 500ºC by the continuous formation of small pinholes.

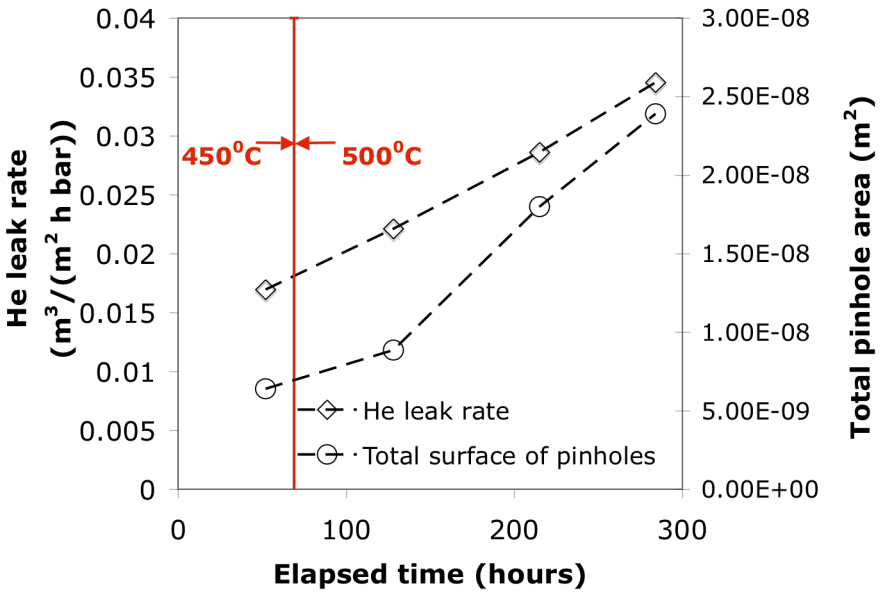

Figure 10-6 He leak rate vs. time at 450ºC and 500ºC for membrane Ma-41. The total pinhole area ($\varepsilon_\alpha \cdot S$) as function of time at 500ºC and 550ºC was also plotted.

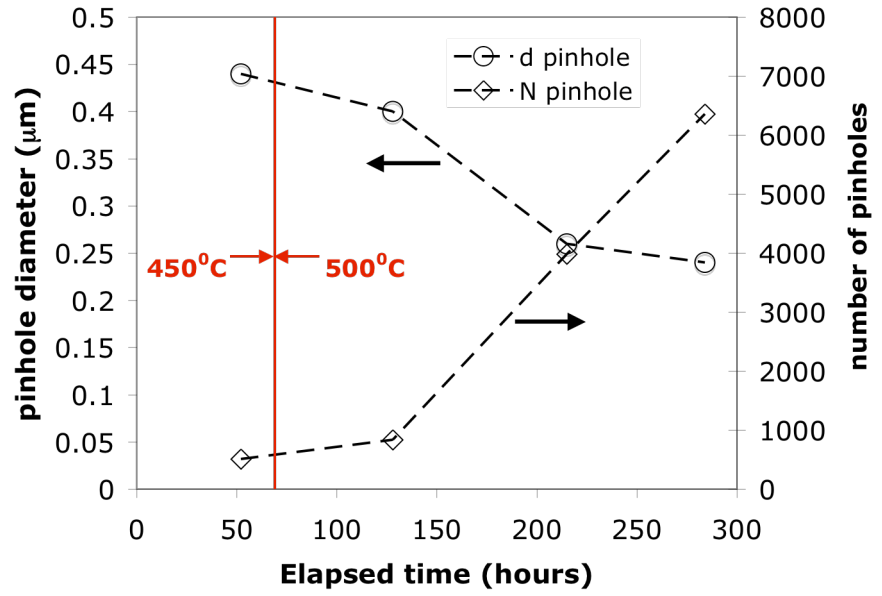

Figure 10-7 Pinhole diameter and number of pinholes as a function of time at 450ºC and 500ºC.

Figure 10-8 shows the He permeance and the total pinhole area for membrane Ma-34b as a function of time at 500 and 550ºC. the total pinhole area ($\varepsilon_\alpha \cdot S$) as a function of time was calculated using the data in Figure 10-5 and Equations (10-3) to (10-5). At 500ºC the leak rate increased linearly with time yet the total pinhole area appeared to be constant.

At 550ºC both the leak rate and the total pinhole area rapidly increased. Figure 10-9 shows the average pinhole diameter and the total number of pinholes in the 120 cm^2 of membrane Ma-34b as a function of time at 500ºC and 550ºC. The average pinhole diameter and the total number of pinholes were also estimated using data in Figure 10-5 and Equations (10-3), (10-4b) and (10-5). The average pinhole diameter increased as a function of time. It appeared then that at 500ºC the increase in He permeance was only due to an increase in pinhole size since the total pinhole surface and also the total number of pinholes were relatively constant. When the temperature was raised to 550ºC, the total number of pinholes increased from 100 to 8000. Also, the average pinhole size decreased from 0.8-1 μm to 0.4 μm. Therefore, The increase of the leak at 550ºC occurred by the formation of a large number of new pinholes with an average diameter of 0.35 μm.

In both membranes, Ma-34b and Ma-41, the average pinhole size decreased while the total number of pinholes increased when a temperature change was performed (450-500ºC or 500-550ºC) indicating the formation of new and small pinholes. The main difference between the two membranes was that in the case of Ma-41, the increase in total pinhole number was slow, while for membrane Ma-34b the total pinhole number increased by a factor of a 1000 in only 60 hr. In addition, Figure 10-6 suggests that at 500ºC formation and growth of pinholes occurred at the same time.

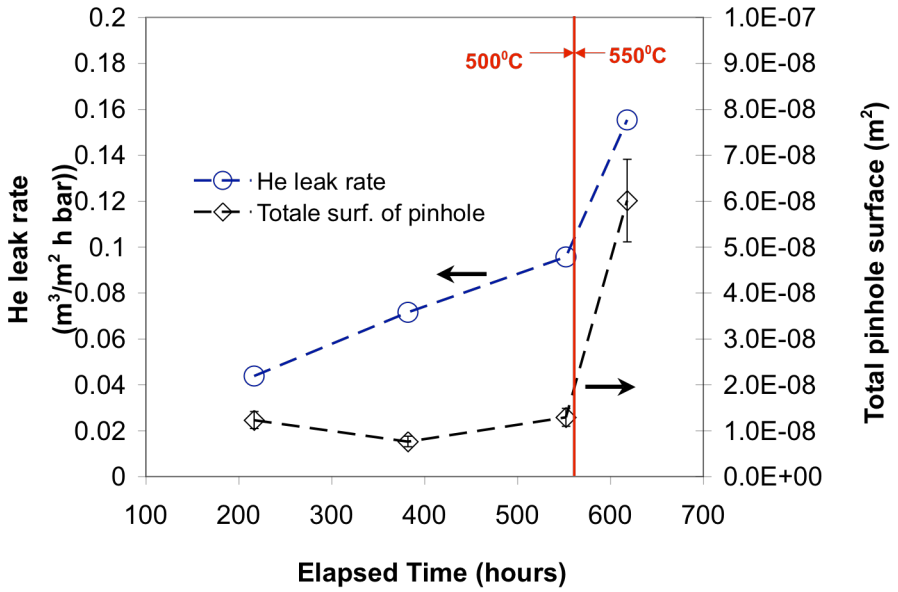

Figure 10-8 He leak rate vs. time at 500ºC and 550ºC for membrane Ma-34b. The total pinhole area ($\varepsilon_\alpha \cdot S$) as function of time at 500ºC and 550ºC was also plotted.

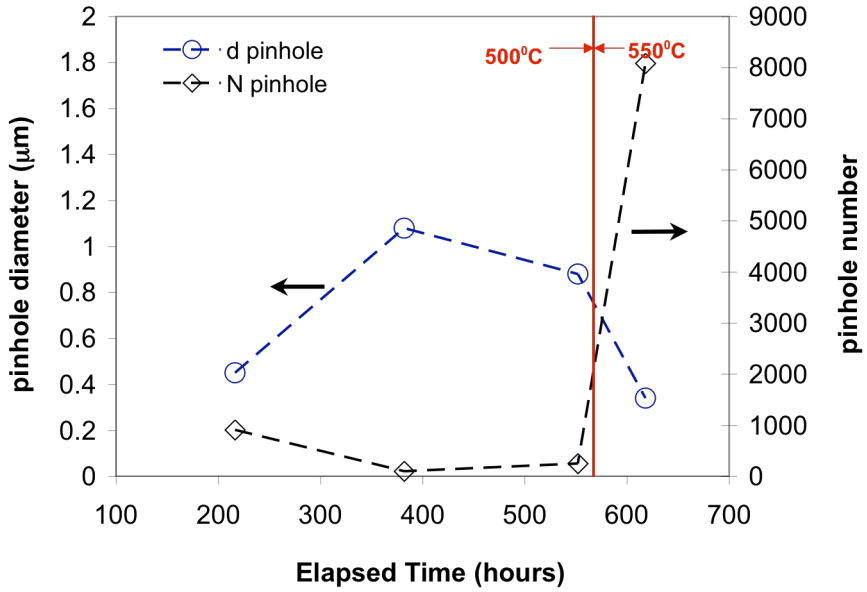

Figure 10-9 Pinhole diameter and number of pinhole as a function of time at 450ºC and 500ºC.

10.3.1.4 Distribution of defects in composite Pd membranes

Knowing the leak distribution in the membrane was an important piece of information to understand whether the He leak was due to localized imperfections or due to a process affecting the entire surface of the membrane.

In order to locate the He leak of Ma-32b and Ma-32c a rising "water test" was performed after cooling the membrane down to room temperature. The rising "water test" was performed according to the procedure described in Section 3.3.2. The normalized He leak for Ma-32b and Ma-32c were plotted in Figure 10-10 as a function of the water level. The He leak of Ma-32b/32c membranes decreased rather uniformly as the water level was increased, indicating that the He leak of both membranes was distributed uniformly across the surface. Therefore, the process leading to the leak formation and leak growth affected the entire Pd layer. The uniformity character of this process suggested that the leak formation was an internal phenomenon related to the nature of Pd metal.

10.3.2 Kinetics of leak increase in H_2 atmosphere

It is of great interest to determine the temperature at which leaks appeared. The temperature at which the He leak started shed some light on the mechanism of the leak formation. Figure 10-11 shows the He leak of membranes C01-F11a/11b, Ma-41 and Ma-42. For all membranes, the first large increase in He leak was measured at 450ºC, which fell within the range of 0.2-0.4 of the Pd melting point[1] in Kelvin.

[1] Pd melting point: 1552ºC

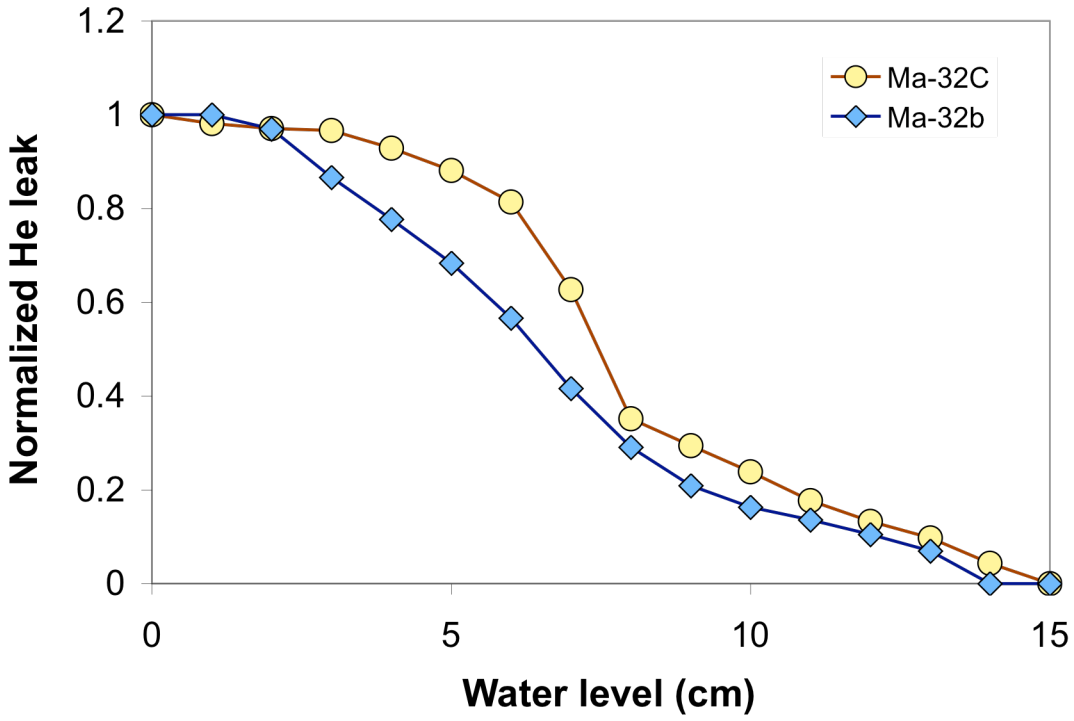

Figure 10-10 He leak as a function of water level for membrane Ma-32b/32c. The "0" mark corresponds to the lower weld and the "15" mark corresponds to the upper weld.

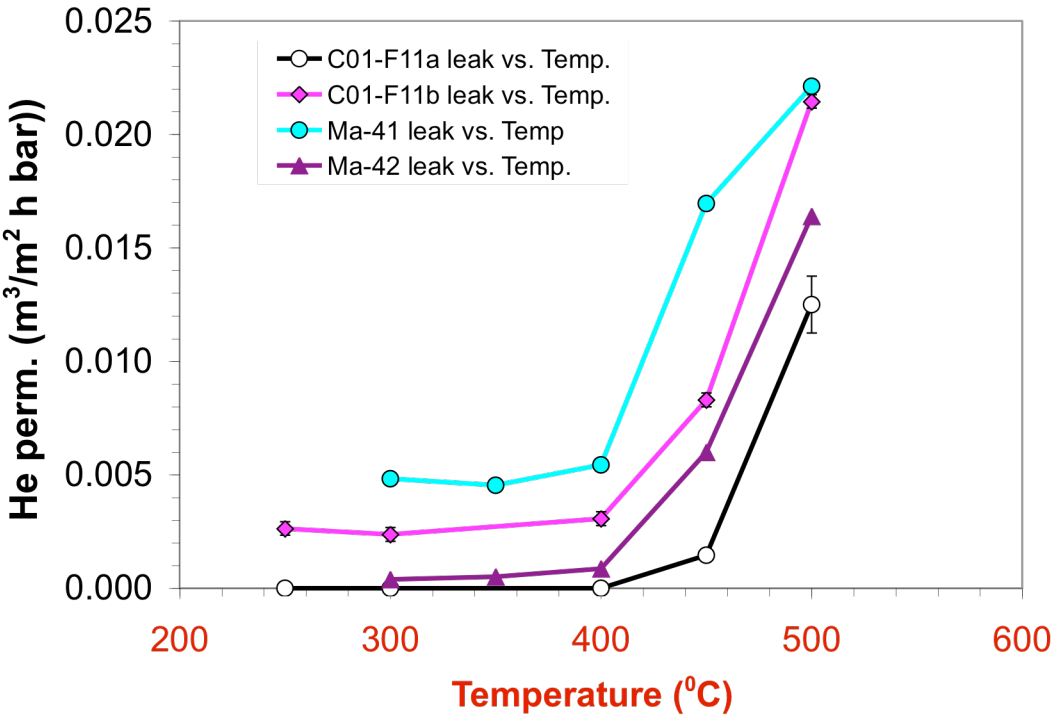

Figure 10-11 He leak of membranes C01-F11/11b and membrane Ma-41 and Ma-42 as a function of temperature.

It has been shown that sintering in nanocrystalline metals starts at 0.2-0.4 of the melting point (Koch, 2002). Therefore, leak formation and leak growth are related to the sintering of Pd grains and Pd clusters.

When plotting the He leak as a function of temperature, it is implicitly assumed that the He leak did not grow with time at a given temperature, which was valid at temperatures lower than 450ºC where the rate of increase of the He leak was very slow. However, at temperatures equal to or higher than 450ºC, the He leak increased faster, and the leak was followed as a function of time at a given temperature. As a consequence, the time for which each membrane was held at each temperature in Figure 10-11 needed to be considered. In fact, the He leak vs. temperature plot shown in Figure 10-11 lacks the "time" variable. The He leak at 450ºC for membrane Ma-41 was almost equal to the He leak at 500ºC because the times at which measurements were taken were not the same. The leak at 450ºC was taken after 500 hr in H_2 while the leak at 500ºC was measured after only 60 hr in H_2 at 500ºC.

Figure 10-12 shows the He leak- He leak$_0$[1] increase in H_2 atmosphere as a function of time for membrane Ma-34b at 450, 500 and 550ºC. The He leak increase was linear as a function of time and the rate of increase for the He leak was determined from the slope at each temperature. A similar approach was used for all composite Pd membranes, when the He leak was measured several times at a given temperature (Ma-32b, Ma-34b and Ma-41).

[1] He leak$_0$ corresponds to the He leak at the time t=0.

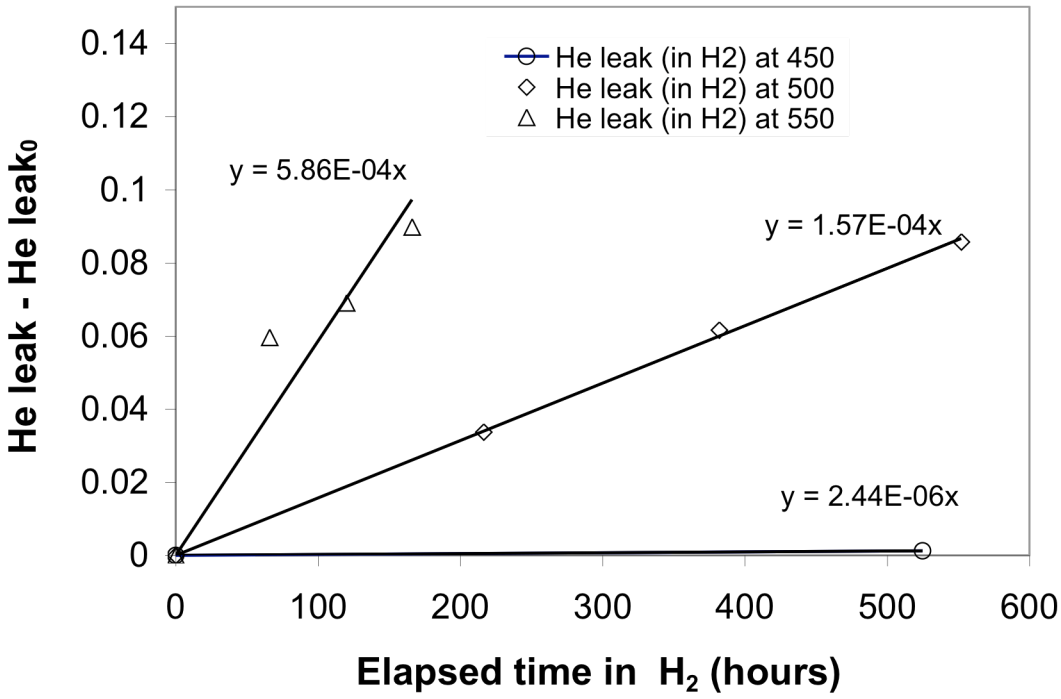

Figure 10-12 He leak rate increase in H_2 atmosphere at 450, 500 and 550ºC for membrane Ma-34b.

The rate of increase for the He leak of membrane C01-F11a/11b and Ma-42 was estimated as described in Section 10.2.3 since only one He leak measurement was performed at each temperature. The natural logarithm of the rate of increase for the leak was then plotted as a function of inverse temperature (Arrhenius plot) in order to estimate the activation energy of the mechanism underlying the leak increase in composite Pd membranes. The Arrhenius plot of leak rate growth for membranes C01-F11a/11b and membranes Ma-32b, Ma-34b, Ma-41 and Ma-42 is shown in Figure 10-13.

Figure 10-13 clearly shows that the rate of increase for the He leak in the 250-400ºC temperature range was very slow and that significant leaks began to develop at 450ºC. Moreover, the rate at which the He leak increased at 500ºC in pure H_2 was similar for all membranes with an average value of $9.1 \cdot 10^{-5}$ $m^3/(m^2\ h\ bar)/h$. Since leaks hardly grew in the 250-400ºC temperature range, the activation energy for leak growth was only estimated in the 450-550ºC temperature range using the rate at which the leak increased for membranes C01-F11a/11b and Ma-32b, Ma-34b and Ma-42. The data of membrane Ma-41, composite Pd-Cu membrane, were omitted for the calculation of the activation energy, as well as the average rate at which the He leak increased at 500ºC. Data for membrane Ma-41 was plotted in Figure 10-11 and Figure 10-13 for comparison purposes only and for later discussions.

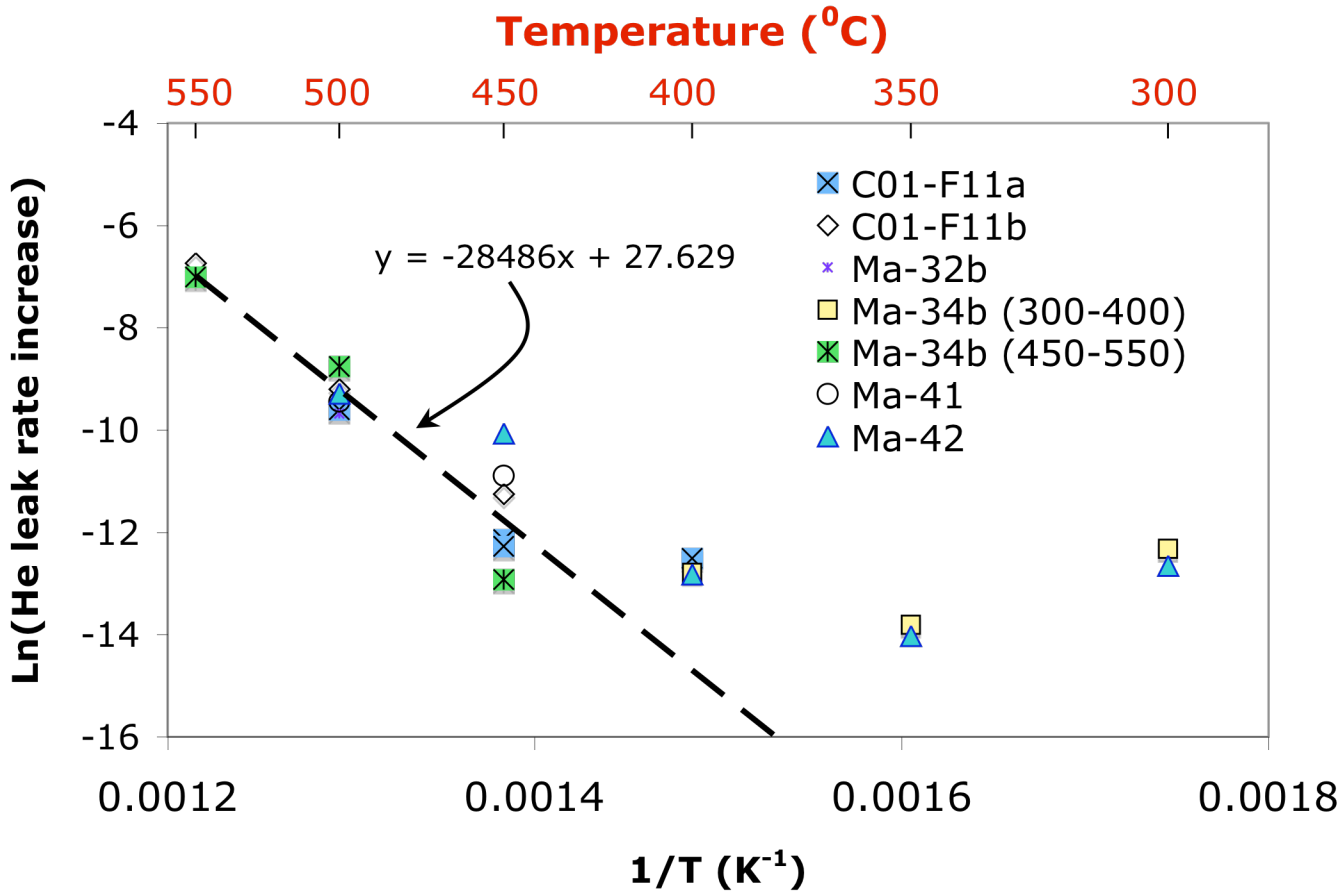

Figure 10-13 Arrhenius plot for membranes C01-F11a/11b and membranes Ma-32b, Ma-34b, Ma-41 and Ma-42. The activation energy was estimated in the 450-550°C temperature range.

The activation energy for the rate of increase was estimated to be 237 kJ·mol^{-1}, which closely matched the activation energy of Pd self diffusion coefficient of 266 kJmol^{-1}. Hence, leak growth was a diffusion-limited process, which required the diffusion of Pd atoms.

10.3.3 Leak growth in He atmosphere

In order to investigate the leak behavior of composite Pd membranes in H_2 and He, the He leak of membrane Ma-34b was measured as a function of time at 500ºC in both He and H_2 atmospheres. After storage and after 500 hr in H_2 at 450ºC, the He leak was measured (0.00285 m^3/(m^2 h bar)). The 450-500ºC temperature change was performed in He atmosphere (ΔP=1 bar) at a rate of 1ºC/min. The He leak did not grow during the temperature change. Therefore, at zero time at 500ºC, the He leak also equaled 0.00285 m^3/(m^2 h bar). After the temperature change, membrane Ma-34b was held in He atmosphere at 500ºC for 1,500 hr and the leak was monitored as a function of time. After 1,500 hr in He, H_2 was introduced for 500 hr. The leak which developed in H_2 atmosphere was measured three times by switching briefly back to He atmosphere. A similar procedure was used at 550ºC to measure the rate of increase in the He leak at 550ºC. The H_2 permeance of membrane Ma-34b at 450ºC was 24 m^3/(m^2 h bar$^{0.5}$) and was expected to be 28 m^3/(m^2 h bar$^{0.5}$) at 500ºC. However, after 1,500 hr in He at 500ºC the H_2 permeance was only 10 m^3/(m^2 h bar$^{0.5}$) and increased to 20 m^3/(m^2 h bar$^{0.5}$) after 350 hr in H_2 at 500ºC.

Industrial He contains some impurities (O_2, CO, CO_2) that were adsorbed on the surface of the Pd layer during the time the membrane was kept at 500ºC in He resulting in a very low H_2 permeance at 500ºC. The process was partially reversible since part of the

expected H_2 permeance (28 $m^3/(m^2\ h\ bar^{0.5})$) was recovered by holding the membrane in pure H_2 at 500ºC.

Figure 10-14 shows the He leak –He $leak_0$ of membrane Ma-34b at 500ºC in He atmosphere. The He leak started to increase after 300 hr following an "S" curve, characteristic of nucleation and growth processes. After 900-1000 hr the He leak reached a steady value equal to 0.0093 $m^3/(m^2\ h\ bar)$. After 1500 hr, H_2 was introduced and the He leak did not show the same pattern as in He atmosphere. The leak in H_2 atmosphere increased linearly ($1.57\ 10^{-4}\ m^3/(m^2\ h^2\ bar)$) and, assuming a linear rate increase in He atmosphere for he first 1000 hr, the leak increased 27 times faster in H_2 atmosphere than in He atmosphere ($5.85\ 10^{-6}\ m^3/(m^2\ h^2\ bar)$). The He leak of membrane Ma-32b as a function of time at 500ºC in H_2 atmosphere was also plotted for comparison purposes. The leak of membrane Ma-32b as a function of time follows a polynomial trend and was characterized by a short induction time of 100 hr.

After the induction time, the rate of increase in the He leak of membrane Ma-32b was considered as linear (last three data points) with a value equal to $8.73\ 10^{-5}\ m^3/(m^2\ h^2\ bar)$, which is close to the He leak increase of membrane Ma-34b at 500ºC in H_2 atmosphere. Therefore, the He leak was considered as linear in both He and H_2 atmosphere, after a short induction time in H_2 (100 hr) and longer induction time in He (300 hr). In He atmosphere, some process inhibited the growth of the leak while in H_2 atmosphere the leak grew continually.

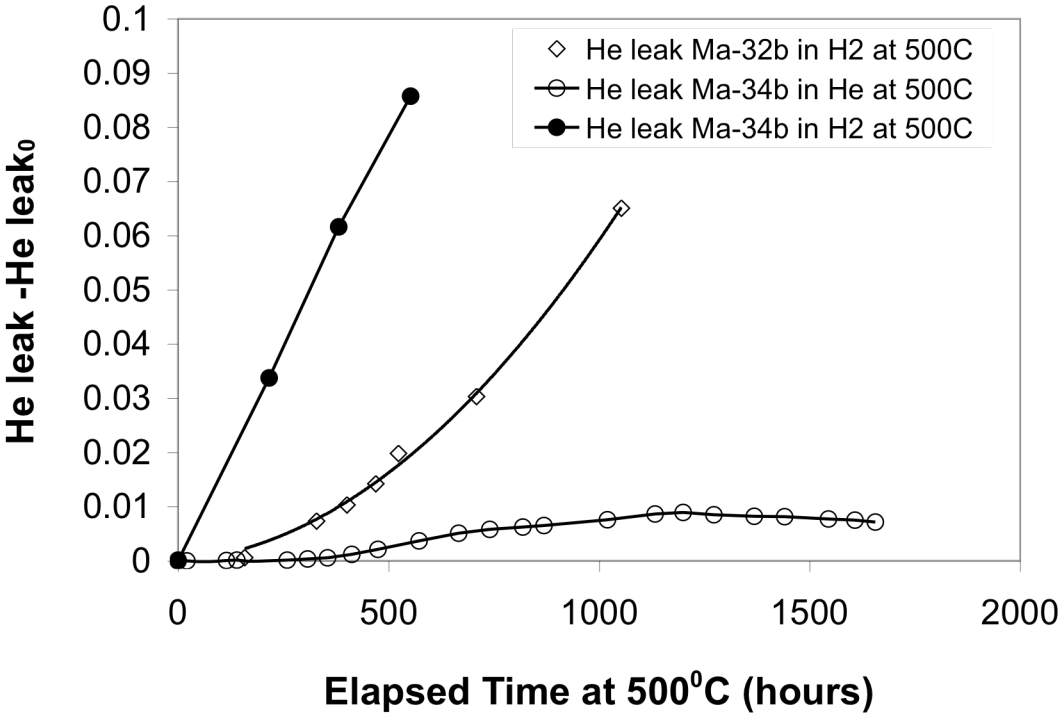

Figure 10-14 He leak increase at 500ºC of membrane Ma-34b in He atmosphere (circles) and in H_2 atmosphere (filled circles). The He leak increase of membrane Ma-32c at 500ºC in H_2 atmosphere was also plotted for comparison purposes.

10.3.4 Leaks in Pd-Cu membranes: the case of Ma-41

As already explained in Sections 2.1 and 7.1, one of the main purposes of alloying Pd with Cu is that the solubility of H_2 in Pd-Cu is very low, therefore, Pd-Cu are less prone to hydrogen stress problems and Pd-Cu alloys would develop less leaks than Pd membranes. It was of great interest to determine the leak stability of membrane Ma-41 at low temperatures (250-400ºC) and especially the leak behavior as a function of time at 450ºC and 500ºC in H_2 atmosphere to compare with composite Pd membranes. The He leak in He atmosphere at 300ºC was equal to 0.0048 $m^3/(m^2$ h bar) (selectivity H_2/He = 1050) after exposure to H_2 at 300ºC. After measuring H_2 permeance at 350 and 400ºC the He leak was measured at 400ºC in He atmosphere and equaled 0.0054 $m^3/(m^2$ h bar) (selectivity H_2/He = 1760). Since the He leak was almost unchanged up to 400ºC it appeared that the membrane microstructure did not change as the temperature was raised i.e. no changes in defects occurred at temperatures between 250 and 400ºC, which was consistent with the fact that the microstructure of composite Pd-PH structures did not change at temperatures lower than 400ºC (Sections 9.4.2.1 and Section 10.3.2). The initial He leak at 450ºC, determined with a GC analysis, equaled 0.0046 $m^3/(m^2$ h bar), which was equal to the He leak at 400ºC within experimental error. That is, the He leak did not increase during the 50 minutes (1ºC/min) of the temperature change. Figure 10-15 shows the He leak rate and selectivity (H_2/He) as a function of time at 450ºC and 500ºC in H_2. The selectivity steadily decreased as a function of time at 450 and 500ºC in H_2.

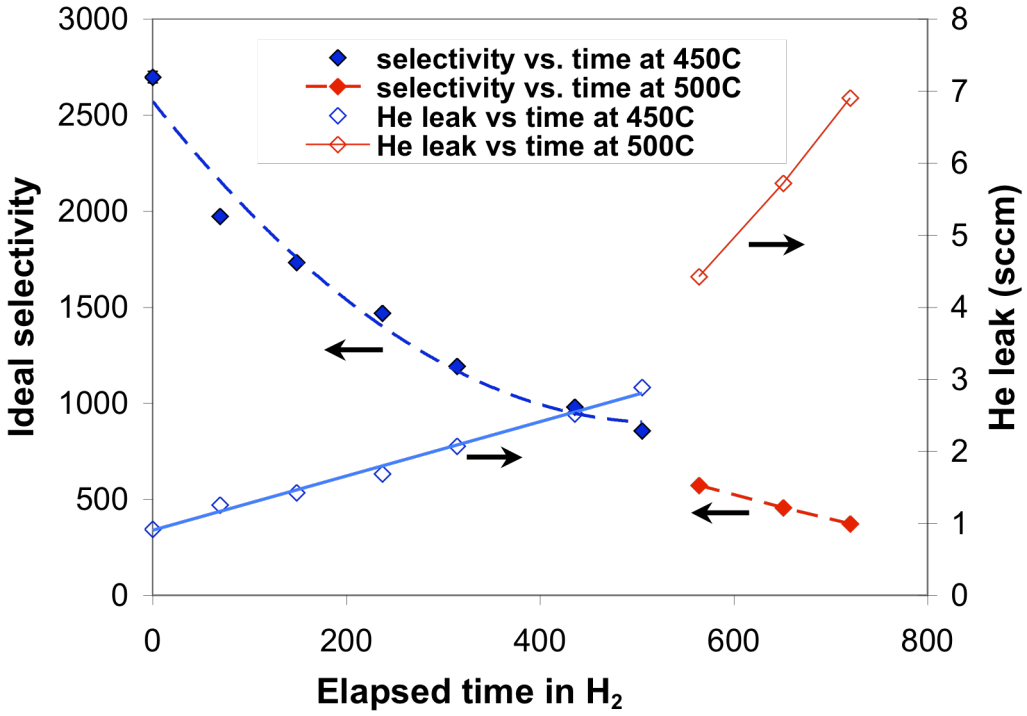

Figure 10-15 Ideal selectivity (H_2/He) and He leak (sccm[1]) as a function of time exhibited by the Pd-6.8wt% Cu membrane at 450°C in H_2 atmosphere

[1] sccm= standard cm^3 per minute

The rate at which the He leak increased was determined and plotted, as already seen, in Figure 10-13. The rate at which the He leak increased in Ma-41 was similar to the rate at which the He leak increased in membranes C01-F11a/11b, Ma-32b/34b/42. It is particularly interesting to note that at 450ºC, composite Pd membranes were under a compressive stress of magnitude around 10 MPa in H_2 atmosphere (see Figure 9-9) and that composite Pd-Cu membranes were most probably under a tensile stress of magnitude around 19 MPa at same conditions (see Figure 9-21). Apparently, the nature of the stress did not have large influences on the rate at which the leak developed in both type of composite membranes. That is due to the fact that stress do not play an important role in leak formation. That is, even though it was possible to lower the magnitude of the compressive stress at 450ºC for the Pd-Cu alloy, leaks still develop and at a similar rate than in Pd membranes. Hence, the reasons for leaks is the sintering of Pd clusters.

10.3.5 The formation of leaks in composite Pd membranes prepared by the electroless deposition technique

All materials keep excess energy in many ways such as stresses, surface energy in grain boundaries and metastable phases. Lower energy states are thermodynamically favorable. Many energy release mechanisms (sintering, dislocations, recrystallization) are diffusion-controlled mechanisms. Since diffusion is slow at low temperatures, materials kept at low temperatures will not undergo structural changes due to kinetics limitations (diffusion). At higher temperatures, when the activation energy for nucleation is overcome, diffusion is fast and the transformations occur. Fresh electroless Pd deposits were also characterized by an excess of energy since they were slightly porous and included a

significant number of Pd clusters (0.5μm) each one of which composed of thousands of 100nm Pd crystallites.

Moreover, fresh electroless Pd deposits are characterized by initial "intrinsic" tensile stresses and extrinsic stresses due to H_2 loading and Pd/support thermal coefficient mis-match. Therefore, electroless Pd deposits will undergo structural modifications at high temperatures i.e. at temperatures close to the Tamman temperature of Pd (m.p./2 in K), where Pd atoms acquire sufficient mobility. Section 9.4.2.3 showed that the temperature at which stress relaxation occurred was close to 400-450ºC and Section 0 showed that leaks started to develop at 400-450ºC. Section 10.3.2 showed that the leak development was a diffusion limited process with a high activation energy. Since the leak formation is a diffusion-limited process, any parameter affecting the diffusion of Pd atoms will have an impact on leak formation.

The Pd self-diffusion is a substitutional diffusion mechanism, that is, in order for a Pd atom to diffuse it needs first to overcome an activation barrier. Figure 10-16(a) depicts the jump of a Pd atom into a vacancy in a plane and Figure 10-16(b) depicts the jump of a Pd atom in a fcc cell (Porter and Easterling, 1981). In both cases, the jump of a Pd atom into a vacancy requires the stretch of other Pd atoms in between the Pd atom of interest and the vacancy. The absorption of H_2 leads to expansion of the Pd lattice cell, therefore the energy the Pd atom needs to overcome to jump into the vacancy is lower when H is dissolved in Pd. Indeed, Pd atoms 1 and 2 in Figure 10-16(a) are already stretched in H_2 atmosphere. Moreover, H_2 absorption leads to the increase of vacancies in Pd. Therefore, Pd self-diffusion coefficient is increased in H_2 atmosphere causing a faster leak growth in H_2 atmosphere than in He atmosphere as experimentally seen (see Figure 10-14)

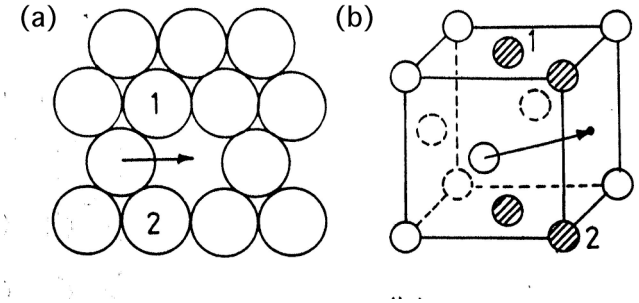

Figure 10-16 Jump into a vacant site. (a) Atoms 1 and 2 need to stretch. (b) The four dashed atoms need to stretch in the fcc cell (Porter and Easterling, 1981).

The process leading to the growth of Pd crystallites (see Figure 9-3(e)(f)) is sintering. The *sintering rate* is equal to the product of *mobility* and *stress* or *driving force,* which for sintering is defined as the surface energy times the surface curvature and is given by Equation (10-6)

$$\sigma_l = \gamma \cdot g \cdot (\frac{1}{R_1} + \frac{1}{R_2}) \qquad (10\text{-}6)$$

where γ is the interfacial energy, g a geometric constant, R_1 and R_2 are the curvature radii at the surface. For spherical particles R_1 and R_2 are equal and g equals to 1. Hence, smaller particles lead to higher stresses and faster sintering rates. Mobility refers to the speed of the process involved during sintering. Processes may be: surface diffusion (predominant at low temperatures), volume diffusion, grain boundary diffusion, plastic flow (when microstructure is highly curved) and dislocation climb. Electroless Pd deposits are characterized by a relatively high driving force for sintering due to their fine grain structure (100 nm Pd crystallites). The release of stresses at 400-450ºC (Section 9.4.2.3) and Figure 9-4 indicated that sintering started at 400-450ºC.

Sintering can occur coherently and incoherently (Skorokhod, 2003). Coherent sintering leads to a homogenous and high-density (close to or equal to the bulk material) material. However, incoherent sintering leads to evolution of pores and microholes due to local densification or differential shrinkage. Differential shrinkage is characteristic of sintering in ultra-fine materials. Coherent and incoherent sintering are depicted in Figure 10-17 from simulations performed by Skorokhod (2003).

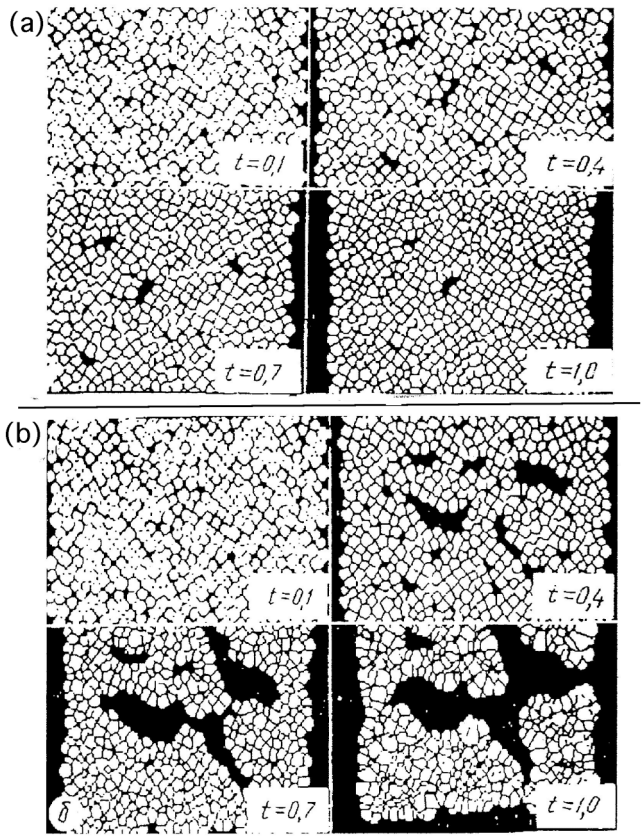

Figure 10-17 Mathematical simulation of (a) coherent sintering and (b) incoherent sintering (Skorokhod, 2003)

Figure 10-17(a) shows a simulation of the coherent sintering of small particles at different times. Figure 10-17(b) shows a simulation of the incoherent sintering of small particles at different times. Incoherent sintering leads to the formation of local voids.

It is known that the sintering process of metals depends on the sintering atmosphere. Indeed, faster densification was obtained for martensic steels in a 60%H_2-40%N_2 mixture than in pure N_2 (Blaine et al., 2003). H_2 reduced surface oxides formed at the grain boundaries increasing grain boundary mobility and therefore decreasing sintering time. It was possible that a thin oxide film at the Pd grain boundaries inhibited the grain growth or Pd cluster sintering in He atmosphere. However, the thin oxide layer was reduced in the presence of H_2 leading to incoherent sintering, leak formation and leak growth.

10.4 Conclusions

Raising water tests on Ma-32 showed that leaks in Pd membranes were uniformly distributed on the surface. Pinhole formation was faster at 550ºC than at 500ºC. The leak growth was found to be to diffusion-limited process with an activation energy equal to 237 kJ mol^{-1}, which corresponded to the activation energy of Pd self-diffusion coefficient. The fact that the leak growth was a diffusion-limited process was in agreement with the finding that leaks grew faster in H_2 atmosphere. Indeed, absorbed H in the Pd increases the self-diffusion coefficient of Pd. Pinhole formation at temperatures higher than 450ºC was due to incoherent sintering of the small (100nm) Pd crystallites.

.

11 Conclusions

- A new technique using pre-activated Al_2O_3 particles of different sizes was developed to grade the porous metal supports to obtain a very smooth surface with a narrow pore size distribution. The composite Pd membranes achieved on graded porous metal supports were as thin as 5.6 μm.
- The H_2 permeance of composite Pd and membranes prepared on graded PH supports was as high as 50 $m^3/(m^2\ h\ bar^{0.5})$. H_2 permeances as high as 93 $m^3/(m^2\ h\ bar^{0.5})$ were expected however, the presence of mass transfer within the porous support strongly affected the H_2 permeance.
- The H_2 permeance of composite Pd membranes prepared on graded PH supports was stable over 1100 hr at 500ºC in H_2 atmosphere.
- The H_2 permeance was enhanced by the oxidation of the membrane surface at 350ºC for 48 hr.
- The selectivity (H_2/He) of composite Pd membranes prepared on graded supports was higher than 300 for periods of time over 1100 hr at 500ºC in H_2 atmosphere. The selectivity of all membranes at temperatures lower than 400ºC was as high as 1000.
- Pd-Cu membranes prepared on graded supports showed permeances as high as 30 $m^3/(m^2\ h\ bar^{0.5})$ at 450ºC with a selectivity (H_2/He) equal to 900.

- The ordering transformation fcc→bcc occurred with the fastest rate at 400-450ºC with a 50% conversion after only 60 seconds.
- Thin Pd films deposited with the electroless deposition method were characterized by a nanocrystalline structure with Pd crystallites of 50-100 nm.
- It was found that, at low temperatures, part of the H_2 permeating through the composite Pd membranes, diffused through Pd grain boundaries.
- Microstrains and initial intrinsic stresses release occurred at 400ºC without visible sintering of Pd clusters. The release of microstrains and initial intrinsic stresses did not affect membrane selectivity.
- At temperatures higher than 400ºC, the energy was sufficient for thermal stresses to be released, which occurred with significant sintering of Pd grains and clusters.
- PH supports were more suited for the preparation of composite Pd membranes. The presence of a thick Cr_2O_3 layer drastically inhibited intermetallic diffusion at 500ºC. The Cr_2O_3 layer was not reduced in H_2 atmosphere and high temperatures (600ºC). All PH supports had a large mass transfer resistance.
- A model was developed to predict the effect of mass transfer resistance within the porous support of composite Pd membranes on the H_2 permeation mechanism. The activation energy for H_2 permeation data of all membranes were in good agreement with the mass transfer model.
- For the first time, the kinetics of H_2 flux decline were measured and showed that, at temperatures lower than 500ºC intermetallic diffusion occurred by the diffusion of Fe through Pd grain boundaries. At temperature higher than

500ºC, intermetallic diffusion took place by the diffusion of Fe through the Pd lattice.

- For the first time, the kinetics of selectivity decline were measured and showed that, leak growth was a diffusion-limited process and was attributed to the in-coherent sintering of Pd nano-crystallites.
- Thermal stresses and hydrogen stresses had no influence on selectivity decline.

12 Recommendations

In order to achieve composite Pd membranes with higher H_2 permeance and even better long-term stability, further research should focus on:

- The use of porous metal supports having a larger He permeance than PH supports in order to avoid mass transfer limitations.
- Develop thinner and more stable barriers for the inhibition of the intermetallic diffusion phenomena. The formation or deposition of the barrier should not lead to a large decrease of the He permeance of the bare support to avoid mass transfer limitations.
- The study of other smoothing techniques such as deposition of γ-alumina by the sol gel method. very smooth surfaces can be achieved by first grading the support with pre-activated Al_2O_3 particles followed by a thin (0.2-0.4 μm) of a sol gel layer.
- A further study on Pd surface modification is needed. The deposition of a thin layer of Pd black may lead to the increase of the H_2 permeance. If so, investigate the reasons for the increase in H_2 permeance.
- The study of the sintering mechanism of electroless thin Pd deposits by in-situ electron microscopic techniques. This experiment will further substantiate the incoherent sintering mechanism.

- The synthesis of Pd-Cu membranes having 40-42 wt% Cu on engineered surfaces.
- The study of the ordering/disordering transformation in a composite Pd -40 wt% Cu membrane on the leak stability of the membrane.

To avoid the sintering of Pd nano-crytsallites two approaches can lead to similar results: start from the beginning with a membrane having large Pd grains (no surface excess energy) or, freeze the initial microstructure. The following experiments are of great importance

- Study a composite Pd membrane with no excess energy to avoid incoherent sintering. A composite Pd membrane with no excess energy can be prepared by sputtering deposition (or CVD) and by heating the support at a temperature of 450ºC during deposition. The leak of this composite Pd membrane should not grow.
- Harden Pd with refractory metals to reduce the mobility of grain boundaries thereby, decreasing the sintering rate. This idea is based on the Zenner pinning effect of grain boundaries, which is commonly seen in metallographic studies.

References

Abys, J. A. (1964). U.S patent 4,424,241.

Aggarwal, S., A. P. Monga, S. R. Perusse, R. Ramesh, V. Ballarotto, E. D. Williams, B. R. Chalamala, Y. Wei and R. H. Reuss (2000). "Spontaneous ordering of oxide nanostructures." *Science* 287.

Akis, B. C., E. E. Engwall, P. I. Mardilovich and Y. H. Ma (2003). "Effects of the in-situ formation of an intermetallic diffusion barrier layer on the properties of composite palladium membranes." *American Chemical Society, Preprints* 48(1): 337-338.

Ali, J. K., E. J. Newson and D. W. T. Rippin (1994). "Deactivation and regeneration of Pd-Ag membranes for dehydrogenation reactions." *Journal of Membrane Science* 89(1-2): 171.

Athayde, A. L., R. W. Baker and P. Nguyen (1994). "Metal composite membranes for hydrogen separation." *Journal of Membrane Science* 94(1): 299.

Babanov, Y. A., L. A. Blaginina, I. V. Golovshchikova, T. Haubold, F. Boscherini and S. Mobilio (1997). "Defects in nanocrystalline palladium." *The physics of metals and metallography* 83(4): 444-451.

Balovnev, Y. A. (1974). "Diffusion of hydrogen in palladium." *Russian Journal of Physical Chemistry* 48(3): 409-410.

Baranowski, B., S. Majchrzak and T. B. Flanagan (1971). "The volume increase of fcc metals and alloys due to interstitial hydrogen over a wide range of hydrogen contents." *j. Phys. F: Metal Phys.* 1: 258-261.

Bartlett, A. A. (2000). "An analysis of U.S and world oil production patterns using Hubbert style curves." *Mathematical Geology* 32(1).

Blaine, D. C., Y. Wu, C. E. Schlaefer, B. Marx and R. M. German (2003). "Sintering shrinkage and microstructure evolution during densification of a martensitic stainless steel."

Bogdanov, S. V., E. M. Moroz and S. V. Tsylbulya (1984). "Investigation of substructure of catalysts by x-ray diffractions methods." *Kinetics and Catalysis* 25(5): 1028-1032.

Brandes, E. A. and G. B. Brook (1998). *Smithells Metals Reference Book (7th Edition)*, Elsevier.

Brodowsky, H. and E. Poeschel (1965). *Z. phys. Chem. N.F* 44: 143.

Bryden, K. J. and J. Y. Ying (2002). "Nanostructured palladium-iron membranes for hydrogen separation and membrane hydrogenation reactions." *Journal of Membrane Science* 203: 29-42.

Campbell, J. C. and J. H. Laherrere (1998). "The end of cheap oil." *Scientific American* 278(3): 78-83.

Checchetto, R., N. Bazzanella, B. Patton and A. Miotello (2004). "Palladium membranes prepared by r.f. magnetron sputtering for hydrogen purification." *Surface and Coatings Technology* 177-178: 73-79.

Cheng, Y. S., M. A. Pena, J. L. Fierro, D. C. W. Hui and K. L. Yeung (2002). "Performance of alumina, zeolite, palladium, Pd-Ag alloy membranes for hydrogen separation from Towngas mixture." *Journal of Membrane Science* 204(1-2): 329.

Cheng, Y. S. and K. L. Yeung (2001). "Effects of electroless plating chemistry on the synthesis of palladium membranes." *Journal of Membrane Science* 182(1-2): 195.

Collins, J. P. and J. D. Way (1993). "Preparation and characterization of a composite Palladium-ceramic membrane." *Ind. Eng. Chem. Res.* 32: 3006-3013.

Collins, S. R. (1998). "Stainless steel for semi-conductor applications." *Mechanical working and steel processing conference proceedings*(35): 607-619.

Cullity, B. D. and S. R. Stock (2001). *Elements of x-ray diffraction*. Upper Saddle River, NJ, Prentice Hall, Edition: 3rd ed.

Davis, W. (1954). *USAEC Report KAPL-1227, U. S. Atomic Energy Commission*.

Dirks, A. G. (1977). "Columnar microstructure in vapor-deposited thin films." *Thin Solid Films* 49: 219.

Duncan, R. C. and W. Youngquist (1999). "Encircling the peak of world oil production." *Natural Resources Research* 8(3): 219-232.

Eastman, J. A., L. J. Thompson and B. J. Kestel (1993). "Narrowing of the palladium-hydrogen miscibility gap in nanocrystalline palladium." *Physical Review B* 48(1): 84-92.

Edlund, D. J. and J. McCarthy (1995). "The relationship between intermetallic diffusion and flux decline in composite-metal membranes: implications for achieving long membrane lifetime." *Journal of Membrane Science* 107(1-2): 147.

Edlund, D. J. and W. A. Pledger (1993). "Thermolysis of hydrogen sulfide in a metal-membrane reactor." *Journal of Membrane Science* 77(2-3): 255.

Edlund, D. J. and W. A. Pledger (1994). "Catalytic platinum-based membrane reactor for removal of H_2S from natural gas streams." *Journal of Membrane Science* 94(1): 111.

Edwards, J. D. (1997). "Crude oil and alternative energy forecasts of the twenty-first century. The end of hydrocarbon era." *American Association of Petroleum Geologists Bulletin* 81: 1292-1305.

Farias, D., M. Patting and K. H. Rieder (1997). "Helium diffraction investigations of the transition of chemisorbed hydrogen into subsurfaces sites on palladium surfaces." *Phys. stat. sol. (a)* 159: 255-262.

Farr, J. P. G. and I. R. Harris (1973). U.S. patent 3,713,270.

Fazle Kibria, A. K. M. and Y. Sakamoto (2000). "The effect of alloying of palladium with silver and rhodium on the hydrogen solubility, miscibility gap and hysteresis." *International Journal of Hydrogen Energy* 25(9): 853.

Flanagan, T. B., G. Gross and J. D. Clewley (1977). "Absorption and diffusion of hydrogen in palladium/iron alloys." *Hydrogen in metals: Proceedings of the 2nd international congress, Paris, 6-10 june, 1977*.

Floro, J. A., S. J. Hearne, J. A. Hunter, P. Kotula, E. Chason, S. C. Seel and C. V. Thompson (2001). "The dynamic competition between stress generation and relaxation mechanisms during coalescence of Volmer-Weber thin films." *Journal of applied physics.* 89(9): 4886-4897.

Fort, D., J. P. G. Farr and I. R. Harris (1975). *Journal of less common metals* 39(2): 293.

Frieske, H. and E. Wicke (1973). "Magnetic susceptibility and equilibrium diagram of PdH_n." *Ber. Bunsenges. Physik. Chem.* 77: 48-52.

Galuszka, J., R. N. Pandey and S. Ahmed (1998). "Methane conversion to syngas in a palladium membrane reactor." *Catalysis Today* 46(2-3): 83.

Gao, H., J. Y. S. Lin, Y. Li and B. Zhang (2005). "Electroless plating synthesis, characterization and permeation properties of Pd-Cu membranes supported on ZrO2 modified porous stainless steel." *Journal of Membrane Science* 265(1-2): 142.

Gillespie, L. J. and L. S. Galstaun (1936). "The palladium-hydrogen equilibrium and new palladium hydrides." *Journal of the American Chemical Society* 58: 2565-2573.

Gillespie, L. J. and F. P. Hall (1926). "The palladium-hydrogen equilibrium and palladium hydride." *Journal of the American Chemical Society* 48: 1207-1219.

Graham, T. (1869a). *Proc. R. Soc.* 17: 212.

Graham, T. (1869b). *Proc. R. Soc.* 17: 500.

Gryaznov, V. (2000). "Metal containing membranes for the production of ultrapure hydrogen and the recovery of hydrogen isotopes." *separation and Purification Methods* 29(2).

Gryaznov, V. M., O. S. Serebyannikova and Y. M. Serov (1993). " Preparation and catalysis over palladium composite membranes." *Applied Catalysis A: General* 96: 15-23.

Guazzone, F., M. E. Ayturk and Y. H. Ma (2004). *Effect of intermetallic diffusion barrier on the stability of composite Pd/PSS membranes at high temperatures*. Annual international Pittsburgh Coal Conference, 21st, Japan, Pittsburgh Coal Conference.

Han, J., I.-S. Kim and K.-S. Choi (2002). "High purity hydrogen generator for on-site hydrogen production." *International Journal of Hydrogen Energy* 27(10): 1043.

Han, J., G. Zhu, D. Y. Zemlyanov and F. H. Ribeiro (2004). "Increase of Pd surface area by treatment in dioxygen." *Journal of Catalysis* 225(1): 7.

Hoang, H. T., H. D. Tong, F. C. Gielens, H. V. Jansen and M. C. Elwenspoek (2004). "Fabrication and characterization of dual sputtered Pd-Cu alloy films for hydrogen separation membranes." *Materials Letters* 58(3-4): 525.

Holleck, G. L. (1970). "Diffusion and solubility of hydrogen in palladium and palladium-silver alloys." *The journal of Physical Chemistry* 74(3): 503-511.

Hough, W. V., J. L. Little and K. V. Warheit (1981). U.S patent 4,255,194.

Howard, B. H., R. P. Killmeyer, K. S. Rothenberger, A. V. Cugini, B. D. Morreale, R. M. Enick and F. Bustamante (2004). "Hydrogen permeance of palladium-copper alloy membranes over a wide range of temperatures and pressures." *Journal of Membrane Science* 241(2): 207.

Hunter, J. B. (1960). "A new hydrogen purification process." *Plat. Met. Rev.* 4: 130-131.

IEA (1997). "International Energy Agency. “World energy prospect to 2020”." *Paper prepared for the G8 energy ministers’ meeting Moscow March 31 - April 1*.

Itoh, N., Y. Kaneko and A. Igarashi (2002). "Efficient hydrogen production via methanol steam reforming by preventing back-permeation of hydrogen in a palladium membrane reactor." *Ind. Eng. Chem. Res.* 41(19): 4702-4706.

Itoh, N., S. Niwa, F. Mizukami, T. Inoue, A. Igarashi and T. Namba (2003). "Catalytic palladium membrane for reductive oxidation of benzene to phenol." *Catalysis Communications* 4(5): 243.

Janßen, S., H. Natter, R. Hempelmann, T. Striffler, U. Stuhr, H. Wipf, H. Hahn and J. C. Cook (1997). "Hydrogen diffusion in nanocrystalline Pd by means of quasielastic neutron scattering." *Nanostructured Materials* 9: 579-582.

Jayaraman, V. and Y. S. Lin (1995). "Synthesis and hydrogen permeation properties of ultrathin palladium-silver alloy membranes." *Journal of Membrane Science* 104(3): 251.

Jemaa, N., J. Shu, S. Kaliaguine and B. P. A. Grandjean (1996). "Thin Palladium Film Formation on Shot Peening Modified Porous Stainless Steel Substrates." *Ind. Eng. Chem. Res.* 35(3): 973-977.

Jun, C.-S. and K.-H. Lee (2000). "Palladium and palladium alloy composite membranes prepared by metal-organic chemical vapor deposition method (cold-wall)." *Journal of Membrane Science* 176(1): 121.

Kamakoti, P., B. D. Morreale, M. V. Ciocco, B. H. Howard, R. P. Killmeyer, A. V. Cugini and D. S. Sholl (2005). "Prediction of Hydrogen Flux Through Sulfur-Tolerant Binary Alloy Membranes." *Science* 307(5709): 569.

Kamakoti, P. and D. S. Sholl (2003). "A comparison of hydrogen diffusivities in Pd and CuPd alloys using density functional theory." *Journal of Membrane Science* 225(1-2): 145.

Karpova, R. A. and I. P. Tverdovskii (1959). *J. Scient. Instrum.* 33: 615.

Kawagoshi, S. (1977). Japanese patent (Kokai Tokkyo Koho) 77-733.

Keuler, J. N. and L. Lorenzen (2002). "Developing a heating procedure to optimize hydrogen permeance through Pd-Ag membranes of thickness less than 2.2 mm." *Journal of Membrane Science* 195(2): 203.

Keuler, J. N., L. Lorenzen, R. N. Sanderson and V. Linkov (1977). "Optimizing palladium conversion in electroless palladium plating of alumina membranes." *Plating and surface finishing*: 34-40.

Kikuchi, E. (2000). "Membrane reactor application to hydrogen production." *Catalysis Today* 56(1-3): 97.

Kikuchi, E., Y. Nemoto, M. Kajiwara, S. Uemiya and T. Kojima (2000). "Steam reforming of methane in membrane reactors: comparison of electroless-plating and CVD membranes and catalyst packing modes." *Catalysis Today* 56(1-3): 75.

Klug, H. P., L. E. Alexander and joint author (1954). *X-ray diffraction procedures for polycrystalline and amorphous materials*, New York, Wiley.

Knapton, A. G. (1977). "Palladium alloys for hydrogen diffusion membranes-A review of high permeability materials." *Plat. Met. Rev.* 21: 44-50.

Koch, C. C. (2002). *Nanostructured Materials - Processing, Properties and Potential Applications*, William Andrew Publishing/Noyes.

Koch, R. (1994). "The intrinsic stress of polycrystalline and epitaxial thin metal films." *j. Phys.: Condens. Matter*(6): 9519-9550.

Koffler, S. A., J. B. Hudson and G. S. Ansell (1969). "Hydrogen permeation through alpha-palladium." *Transactions of the Metallurgical Society of AIME* 245: 1735-1740.

Kurman, P. V., I. P. Mardilovich and A. I. Trokhimets (1990). "Behavior of absorbed hydrogen in the Pd/g-Al_2O_3 system." *Russian Journal of Physical Chemistry* 64(3).

Lafferty, E. J., D. J. Macauley, P. V. Kelly and G. M. Crean (1997). "Atomic force microscopy investigation of the morphology of a UV photodefined palladium activation layer on alumina ceramic and the nucleation of electroless copper at the activated sites." *Mat. Res. Soc. Symp. Proc.* 441: 329-334.

Lee, D.-W., Y.-G. Lee, S.-E. Nam, S.-K. Ihm and K.-H. Lee (2003). "Study on the variation of morphology and separation behavior of the stainless steel supported membranes at high temperature." *Journal of Membrane Science* 220(1-2): 137.

Levine, P. L. and K. E. Weale (1960). "The palladium + hydrogen equilibrium at high pressures and temperatures." *Transactions Faraday Society* 56: 357-362.

Lewis, F. A. (1967). *The palladium hydrogen system*, London, New York, Academic Press.

Li, A., W. Liang and R. Hughes (1998). "Characterization and permeation of palladium/stainless steel composite membranes." *Journal of Membrane Science* 149: 259-268.

Li, A., G. Xiong, J. Gu and L. Zheng (1996). "Preparation of Pd/ceramic composite membrane 1. Improvement of the conventional preparation technique." *Journal of Membrane Science* 110(2): 257.

Li, Y. and Y.-T. Cheng (1996). "Hydrogen diffusion and solubility in palladium thin films." *International Journal of Hydrogen Energy* 21(4): 281-291.

Li, Z. Y., H. Maeda, K. Kusakabe, S. Morooka, H. Anzai and S. Akiyama (1993). "Preparation of palladium-silver membranes for hydrogen separation by the spray pyrolysis method." *Journal of Membrane Science* 78: 247-254.

Lin, Y.-M., G.-L. Lee and M.-H. Rei (1998). "An integrated purification and production of hydrogen with a palladium membrane-catalytic reactor." *Catalysis Today* 44(1-4): 343.

Lin, Y.-M. and M.-H. Rei (2000). "Process development for generating high purity hydrogen by using supported palladium membrane reactor as steam reformer." *International Journal of Hydrogen Energy* 25(3): 211.

Lin, Y.-M. and M.-H. Rei (2001). "Study on the hydrogen production from methanol steam reforming in supported palladium membrane reactor." *Catalysis Today* 67(1-3): 77.

Ma, Y. H., B. C. Akis, M. E. Ayturk, F. Guazzone, E. E. Engwall and I. P. Mardilovich (2004). "Characterization of Intermetallic Diffusion Barrier and Alloy Formation for Pd/Cu and Pd/Ag Porous Stainless Steel Composite Membranes." *Ind. Eng. Chem. Res.* 43(12): 2936-2945.

Ma, Y. H. and F. Guazzone (2004). 1021.2013-000 pending.

Ma, Y. H., I. P. Mardilovich and P. P. Mardilovich (2001). "Effects of porosity and pore size distribution of the porous stainless steel on the thickness and hydrogen flux of palladium membranes." *Journal of the American Chemical Society* 46(2).

Ma, Y. H., P. P. Mardilovich and Y. She (1998). *Stability of hydrogen flux through Pd/Porous Stainlees Steel Composite Membranes, Extended abstract*. The Fifth International Conference on Inorganic Membranes, Nagoya, Japan June 22-26.

Ma, Y. H., P. P. Mardilovich and Y. She (2000). Hydrogen gas-extraction module and method of fabrication. U. S. A. 6,152,987.

Mardilovich, P. P., Y. She, Y. H. Ma and M.-H. Rei (1998). "Defect-Free Palladium Membranes on Porous Stainless-Steel Support." *AIChe journal* 44(2): 310.

Marigliano, G., G. Barbieri and E. Drioli (2003). "Equilibrium conversion for a Pd-based membrane reactor. Dependence on the temperature and pressure." *Chemical engineering and processing* 42: 231-236.

Matzakos, A. N., S. L. Wellington, T. Mikus and J. M. Ward (2003). Integrated flameless distributed combustion/steam reforming membrane reactor for hydrogen production and use thereof in zero emissions hybrid power system. U. S. US 2003/0068269 A1.

McCool, B. A. and Y. S. Lin (2001). "Nanostructured thin Palladium-Silver membranes: effects of grain size on gas permeation properties." *Journal of Material Science* 36: 3221-3227.

McKinley, D. L. (1967). U.S patent 3,350,845.

McKinley, D. L. (1969). U.S patent 3,439,474.

Mitacek, P., Jr. and J. G. Aston (1963). "The thermodynamic properties of pure palladium and its alloys with hydrogen between 30 and 300°K." *Journal of the American Chemical Society* 85(2): 137-141.

Mizumoto, S., H. Nawabune, M. Haga and K. Tsuji (1986). *Extended abstracts of papers presented at the 73rd Tech. Conf., Metal Finish. Soc. Japan, 27B-8*: 116.

Morreale, B. D., M. V. Ciocco, R. M. Enick, B. I. Morsi, B. H. Howard, A. V. Cugini and K. S. Rothenberger (2003). "The permeability of hydrogen in bulk palladium at elevated temperatures and pressures." *Journal of Membrane Science* 212(1-2): 87.

Morreale, B. D., M. V. Ciocco, B. H. Howard, R. P. Killmeyer, A. V. Cugini and R. M. Enick (2004). "Effect of hydrogen-sulfide on the hydrogen permeance of palladium-copper alloys at elevated temperatures." *Journal of Membrane Science* 241(2): 219.

Murakami, M. (1991). "Deformation in thin films by thermal strain." *Journal of Vacuum Science and Technology A* 9(4): 2469-2476.

Müller, K. H. (1985). *J. Appl. Physics* 58: 2573.

Mütschele, T. and R. Kirchheim (1987). "Segregation and diffusion of hydrogen in grain boundaries of palladium." *Scripta metallurgica* 21: 135-140.

Nam, S.-E. and K.-H. Lee (2000). "A study on the palladium/nickel composite membrane by vacuum electrodeposition." *Journal of Membrane Science* 170(1): 91.

Nam, S.-E. and K.-H. Lee (2001). "Hydrogen separation by Pd alloy composite membranes: introduction of diffusion barrier." *Journal of Membrane Science* 192(1-2): 177.

Nam, S.-E., S.-H. Lee and K.-H. Lee (1999). "Preparation of a palladium alloy composite membrane supported in a porous stainless steel by vacuum electrodeposition." *Journal of Membrane Science* 153(2): 163.

Nam, S. E. and K. H. Lee (2005). "Preparation and Characterization of Palladium Alloy Composite Membranes with a Diffusion Barrier for Hydrogen Separation." *Ind. Eng. Chem. Res.* 44(1): 100-105.

Ohno, I., O. Wakabayashih and S. Haruyama (1985). "Anodic oxidation of reductants in electroless plating." *J. Electrochem. Soc.: electrochemical science and technology* 132(10): 2323-2330.

Pearlstein, F. and R. F. Weightman (1969). *Plating* 56(10): 1158.

Porter, D. A. and K. E. Easterling (1981). *Phase transformations in metals and alloys*, Van Nostrand Reinhold Company Ltd.

Radzhabov, T. D., L. Y. Alimova, E. Y. Zhukova and F. S. Melkumyan (1980). "Effect of thin-film coatings on the hydrogen permeability of metals." *Russian Journal of Physical Chemistry* 54(11): 1605-1606.

Ragaini, V., R. Giannantonio, P. Magni, L. Lucarelli and G. Leofanti (1994). "Dispersion measurement by the single introduction method coupled with the back-sorption procedure: a chemisorption and TPD study on the different chemisorbed hydrogen species." *Journal of Catalysis* 146: 116-125.

Rajamani, A., B. W. Sheldon, E. Chason and A. F. Bower (2002). "Intrinsic tensile stress and grain boundary formation during Volmer-Weber film growth." *Applied Physics Letters* 81(7).

Reimann, K. and R. Wurschum (1997). "Distribution of internal strains in nanocrystalline Pd studied by x-ray diffraction." *Journal of applied physics.* 81(11).

Reva, O. V. and T. N. Vorob'eva (2002). "Oxidation, Hydrolysis, and Colloid Formation in Storage of SnCl2 Aqueous Solutions." *Russian Journal of Applied Chemistry* 75(5): 700-705.

Rhoda, R. N. (1959a). *Trans. Inst. Metal Finish.* 36: 82.

Rhoda, R. N. (1959b). U.S patent 2,915,406.

Roa, F. and J. D. Way (2005). "The effect of air exposure on palladium-copper composite membranes." *Applied Surface Science* 240(1-4): 85.

Roa, F., J. D. Way, R. L. McCormick and S. N. Paglieri (2003). "Preparation and characterization of Pd-Cu composite membranes for hydrogen separation." *Chemical Engineering Journal* 93(1): 11.

Roshan, N. R., A. P. Mishchenko, V. P. Polyakova, N. I. Parfenova, E. M. Savitsky, E. A. Voitekhova, V. M. Gryaznov and M. E. Sarylova (1983). "The effect of the surface state on the hydrogen permeability and the catalytic activity of palladium alloy membranes." *Journal of less common metals* 89: 423-428.

Rothenberger, K. S., A. V. Cugini, B. H. Howard, R. P. Killmeyer, M. V. Ciocco, B. D. Morreale, R. M. Enick, F. Bustamante, I. P. Mardilovich and Y. H. Ma (2004). "High pressure hydrogen permeance of porous stainless steel coated with a thin palladium film via electroless plating." *Journal of Membrane Science* 244(1-2): 55.

Sanders, P. G., J. A. Eastman and J. R. Weertman (1998). "Pore distributions in nanocrystalline metals from small-angle neutron scattering." *Acta Materialia* 46(12): 4195.

Sanders, P. G., A. B. Whitney, J. R. Weertman, R. Z. Valiev and R. W. Siegel (1995). *Mater. Sci. Eng. A* 204: 7.

Sergienko, A. (1968). U. S. patent 3,418,143.

She, Y. (2000). Composite palladium membranes: synthesis, separation and reaction. Chemical Engineering. Worcester, Worcester Polytechnic Institute. PhD.

Shirasaki, Y. O., Y. Ohta, K. Kobayashi and K. Kuroda (1997). "Development of a hydrogen separation reformer." *Proceedings of the 27th annual meeting of Japan petroleum institute*: 247.

Shu, J., A. Adnot, B. P. A. Grandjean and S. Kaliaguine (1996). "Structurally stable composite Pd-Ag alloy membranes: Introduction of a diffusion barrier." *Thin Solid Films* 286: 72-79.

Shu, J., B. P. A. Grandjean, A. Van Neste and S. Kaliaguine (1991). "Catalytic palladium-based membrane reactors; a review." *The canadian journal of chemical engineering* 69: 1036-1060.

Shukla, S., S. Seal, J. Akesson, R. Oder, R. Carter and Z. Rahman (2001). "Study of mechanism of electroless copper coating of fly-ash cenosphere particles." *Applied Surface Science* 181: 35-50.

Sieverts, A., E. Jurisch and A. Metz (1915). *Z. anorg. allg. Chem.* 92: 329.

Skorokhod, V. V. (2003). *SURFACE RELAXATION AND LOCAL DENSIFICATION IN NANOSIZED SYSTEMS AT ISOTHERMAL SINTERING*. Sintering 2003: An International Conference on the Science, Technology & Applications of Sintering, https://www.mri.psu.edu/conferences/sint03/pdf/Skorokhod_1_3.pdf.

Souleimanova, R. S., A. S. Mukasyan and A. Varma (2000). "Effects of osmosis on microstructure of Pd-composite membranes synthesized by electroless plating technique." *Journal of Membrane Science* 166(2): 249.

Souleimanova, R. S., A. S. Mukasyan and A. Varma (2002). "Pd membranes formed by electroless plating with osmosis: H_2 permeation studies." *AIChe journal* 48(2): 262-268.

Souleimanova, R. S., M. A. S. and A. Varma (2001). "Pd-composite membranes prepared by electroless plating and osmosis: synthesis, characterization and properties." *Separation and Purification Technology* 25(1-3): 79-86.

Su, C., T. Jin, K. Kuraoka, Y. Matsumura and T. Yazawa (2005). "Thin Palladium Film Supported on SiO_2-Modified Porous Stainless Steel for a High-Hydrogen-Flux Membrane." *Ind. Eng. Chem. Res.* 44(9): 3053-3058.

Subramanian, P. R. and D. E. Laughlin (1991). "Cu-Pd (Copper-Palladium)." *Journal of Phase Equilibria* 12(2).

Swansiger, W. A., J. H. Swisher, J. P. Darginis and C. W. Schoenfelder (1976). "Hydrogen permeation palladium-chromium alloys." *The journal of Physical Chemistry* 80(3): 308-312.

Takasu, S., R. Unwin, B. Tesche and A. M. Bradshaw (1978). *Surface Science* 77: 219.

Thomas, S., R. Schafer, J. Caro and A. Seidel-Morgenstern (2001). "Investigation of mass transfer through inorganic membranes with several layers." *Catalysis Today* 67: 205-216.

Thornton, J. A. (1974). "Influence of apparatus geometry and deposition conditions on the structure and topography of thick sputtered coatings." *Journal of vacuum Science and Technology* 11: 666.

Toda, G. (1958). *J. Res. Inst. Catalysis Hokkaido Univ.* 6: 13.

Tong, J., Y. Kashima, R. Shirai, H. Suda and Y. Matsumura (2005a). "Thin Defect-Free Pd Membrane Deposited on Asymmetric Porous Stainless Steel Substrate." *Ind. Eng. Chem. Res.* 44(21): 8025-8032.

Tong, J., Y. Matsumura, H. Suda and K. Haraya (2005b). "Thin and dense Pd/CeO2/MPSS composite membrane for hydrogen separation and steam reforming of methane." *Separation and Purification Technology* 46(1-2): 1.

Tong, J., H. Suda, K. Haraya and Y. Matsumura (2005c). "A novel method for the preparation of thin dense Pd membrane on macroporous stainless steel tube filter." *Journal of Membrane Science* 260(1-2): 10.

Tosti, S. (2003). "Supported and laminated Pd-based metallic membranes." *International Journal of Hydrogen Energy* 28(12): 1445.

Tosti, S., L. Bettinali, S. Castelli, F. Sarto, S. Scaglione and V. Violante (2002). "Sputtered, electroless, and rolled palladium-ceramic membranes." *Journal of Membrane Science* 196(2): 241.

Tosti, S., L. Bettinali and V. Violante (2000). "Rolled thin Pd and Pd-Ag membranes for hydrogen separation and production." *International Journal of Hydrogen Energy* 25(4): 319.

Touloukian, Y. S., R. K. Kriby, R. E. Taylor and P. D. Desai (1977). "Thermal expansion: metallic elements and alloys." *Thermophysical Properties of Matter* 12: 298.

Uemiya, S., I. Koike and E. Kikuchi (1991a). "Promotion of the conversion of propane to aromatics by use of a palladium membrane." *Applied Catalysis* 76(2): 171.

Uemiya, S., T. Matsuda and E. Kikuchi (1991b). "Hydrogen permeable palladium-silver alloy membrane supported on porous ceramics." *Journal of Membrane Science* 56(3): 315.

Uemiya, S., N. Sato, H. Ando, Y. Kude, T. Matsuda and E. Kikuchi (1991c). "Separation of hydrogen through palladium thin film supported on a porous glass tube." *Journal of Membrane Science* 56(3): 303.

Uemiya, S., N. Sato, H. Ando, K. Y., T. Matsuda and E. Kikuchi (1991d). "Separation of hydrogen through palladium thin film supported on a porous glass tube." *Journal of Membrane Science* 56: 303-313.

Vereshchinskii, S. Y., S. B. Kalmykova and N. V. Korovin (1973). *Zashch. Metal.* 9(1): 117.

Vook, R. W. and F. Witt (1965). "Thermally induced strains in evaporated films." *Journal of Applied Physics* 36(7): 2169-2171.

Völkl, J. and G. Alefeld (1978). *Diffusion of hydrogen in metals. Hydrogen in metals, Vol I. Vol 28 of Topics in applied physics*.

Wang, D., J. Tong, H. Xu and Y. Matsumura (2004). "Preparation of palladium membrane over porous stainless steel tube modified with zirconium oxide." *Catalysis Today* 93-95: 689.

Ward, T. L. and T. Dao (1999). "Model of hydrogen permeation behavior in palladium membranes." *Journal of Membrane Science* 153(2): 211.

Warren, B. E. and B. L. Averbach (1950). *X-ray diffraction studies of cold work in metals: solid solutions and grain boundaries*. Cambridge, MA, Massachusetts Institute of Technology, [Dept. of Metallurgy].

Weissmuller, J., J. Loffler and M. Kleber (1995). "Atomic structure of nanocrystalline metals studied by diffraction techniques and EXAFS." *Nanostructured Materials* 6(1-4): 105.

Wellington, S. L., A. N. Matzakos, T. Mikus and J. M. Ward (2003). Integrated flameless distributed combustion/membrane steam reforming reactor and zero emissions hybrid power system. U. S. US 2003/0068260 A1.

Wicke, E. and G. H. Nernst (1964). "Phase diagram and thermodynamic behavior of the system Pd/H_2 and Pd/D_2 at normal temperatures; H/D separations effects." *Ber. Bunsenges. Physik. Chem.* 68: 224-235.

Wieland, I. S., I. T. Melin and I. A. Lamm (2002). "Membrane reactors for hydrogen production." *Chemical Engineering Science* 57(9): 1571.

Williamson, G. K. and W. H. Hall (1953). "X-ray line broadening from filed aluminum and wolfram." *Acta metallurgica* 1: 22-31.

Witt, F. and R. W. Vook (1968). "Thermally induced strains in cubic metal films." *Journal of applied physics.* 39(6): 2773-2776.

Wolf, R. J., M. W. Lee and J. R. Ray (1994). "Pressure-composition of nanocrystalline palladium hydride." *Physical Review Letters* 73(4): 557-560.

Wu, L. Q., N. Xu and J. Shi (2000). "Preparation of a Palladium Composite Membrane by an Improved Electroless Plating Technique." *Ind. Eng. Chem. Res.* 39(2): 342-348.

Yamakawa, K., M. Ege, B. Ludescher and M. Hirscher (2003). "Surface adsorbed atoms suppressing hydrogen permeation of Pd membranes." *Journal of Alloys and Compounds* 352(1-2): 57.

Yan, S., H. Maeda, K. Kusakabe and S. Morooka (1994). "Thin palladium membrane formed in support pores by metal-organic chemical vapor deposition method and application to hydrogen separation." *Ind. Eng. Chem. Res.* 33: 616-622.

Yang, R. P., X. Cai and Q. L. Chen (2001). "Mechanism of hydrogen desorption during palladium brush-plating." *Surface and Coatings Technology* 141(2-3): 283.

Yepes, D., L. M. Cornaglia, S. Irusta and E. A. Lombardo "Different oxides used as diffusion barriers in composite hydrogen permeable membranes." *Journal of Membrane Science* In Press, Corrected Proof.

Yeung, K. L., J. M. Sebastian and A. Varma (1995). "Novel preparation of Pd/Vycor composite membranes." *Catalysis Today* 25: 231-236.

Zabel, H. and B. Hjorvarsson (2001). Hydrogen in thin films and multilayers. *Progress in hydrogen treatment of materials*. V. A. Goltsov**:** 119-146.

Zayats, A. I., I. A. Stepanowa and A. V. Gorodyskii (1973). *Zahch. Metals.* 9(1): 116.

Zhang, J. Y., S. L. King, I. W. Boyd and Q. Fang (1997). "UV light-induced decomposition of palladium acetate films for electroless copper plating." *Applied Surface Science* 109/110: 487.

Zhao, H. and G. Xiong (1999). "Preparation and characterization of Pd-Ag alloy composite membrane with magnetron sputtering." *Science in China (Serie B)* 42(6): 581-588.

Zhao, H. B., K. Pflanz, J. H. Gu, A. W. Li, N. Stroh, H. Brunner and G. X. Xiong (1998). "Preparation of palladium composite membranes by modified electroless plating procedure." *Journal of Membrane Science* 142(2): 147.

Nomenclature

Ea	Activation energy for H_2 absorption reaction (J mol^{-1} or kJ mol^{-1})
Ed	Activation energy for H_2 desorption reaction (J mol^{-1} or kJ mol^{-1})
Ep	Activation energy for H_2 permeation (J mol^{-1} or kJ mol^{-1})
F_{H2}	H_2 permeance derived from the H_2 flux at ΔP = 1bar (2:1) (m^3 m^{-2} h^{-1} $bar^{-0.5}$)
$F_{0.5}$	H_2 permeance derived from least square analysis assuming n=0.5 (m^3 m^{-2} h^{-1} $bar^{-0.5}$)
F_n	H_2 permeance derived from least square analysis adjusting the n-exponent (m^3 m^{-2} h^{-1} bar^{-n})
J	Gas molar flux (mol m^{-2} s^{-1} or m^3 m^{-2} h^{-1})
K	*Sieverts' constant ($bar^{0.5}$, $Torr^{0.5}$)*
K'	*Proportionality constant when the n-exponent is different than 0.5 ($bar^{n\text{-}exponent}$, $Torr^{n\text{-}exponent}$)*
L	Porous support wall thickness (m or μm)
L_{Pd}	Pd membrane thickness (m or μm)
M_i	Molecular weight for *i* compound (kg mol^{-1})
n-exponent	n-exponent or H_2 pressure exponent (-)
n(H/Pd)	Amount of hydrogen dissolved in the bulk of Pd (mol H/ mol Pd)

P_{H2hp}	H_2 partial pressure in retentate, shell or high pressure side (Pa or bars), also noted as P_{shell}
P_{H2lp}	H_2 partial pressure in permeate, tube or low pressure side (Pa or bars), also noted as P_{tube} or P_0
P_{max}	H_2 pressure at which the maximum solubility in the Pd-H a-phase (a-max) is reached (atm)
Q_0	H_2 Pd permeability pre-exponential factor (m^3 m^1 m^{-2} h^{-1} $bar^{0.5}$)
r	Percentage of the leak permeating according to a Knudsen mechanism. $r=\alpha/(\alpha+\beta \cdot P_{ave})$
R	Universal gas constant (8.314 J mol^{-1} K^{-1})
T	Membrane temperature (at the permeate side) K or ^0C

Greek symbols

α	He leak Knudsen component coefficient (m^3 m^{-2} h^{-1} bar^{-1})
β	He leak viscous component coefficient (m^3 m^{-2} h^{-1} bar^{-2})
ε	Porosity of the Pd layer or the porous support
η_i	Viscosity of gas i (Pa s^{-1})

Appendix A: Error analysis on H_2 permeance

It was of great importance in this work to determine confidence intervals for all fitted parameters: H_2 permeance assuming the Sieverts' law, H_2 permeance and n-exponent from non-linear fit. Specially, great care was taken to measure errors on the n-exponent. Confidence intervals of any given measurement are based on the standard deviation and were determined using Equation A.1

$$\mu = \mu^{ave} \pm t(s/\sqrt{A}) \qquad \text{A.1}$$

where μ is the considered quantity, μ^{ave} is the average value of the data set, A is the number of times that the μ quantity was measured, t is a tabulated number depending on the number of degrees of freedom (equal to A-1) and the degree of confidence required. s is the standard deviation. The standard deviation of the H_2 permeance and n-exponent determined from a non-linear fit and the standard deviation of the H_2 permeance determined from a linear fit were estimated by taking the H_2 flux of membrane C01-F05 as a function of $\Delta P^{0.5}$ ten times during steady state at 250ºC. H_2 permeance measurements were spaced in 24-hr intervals. Figure A.1 shows the H_2 permeance and the n-exponent (from non-linear fit) and the H_2 permeance assuming the Sieverts' law (linear fit) as function of time. The standard deviation of H_2 permeance assuming the Sieverts' law was determined to be 0.02 $m^3/(m^2\ h\ bar^{0.5})$, see Table A.1, attesting to the very good precision achieved in the experimental measurements.

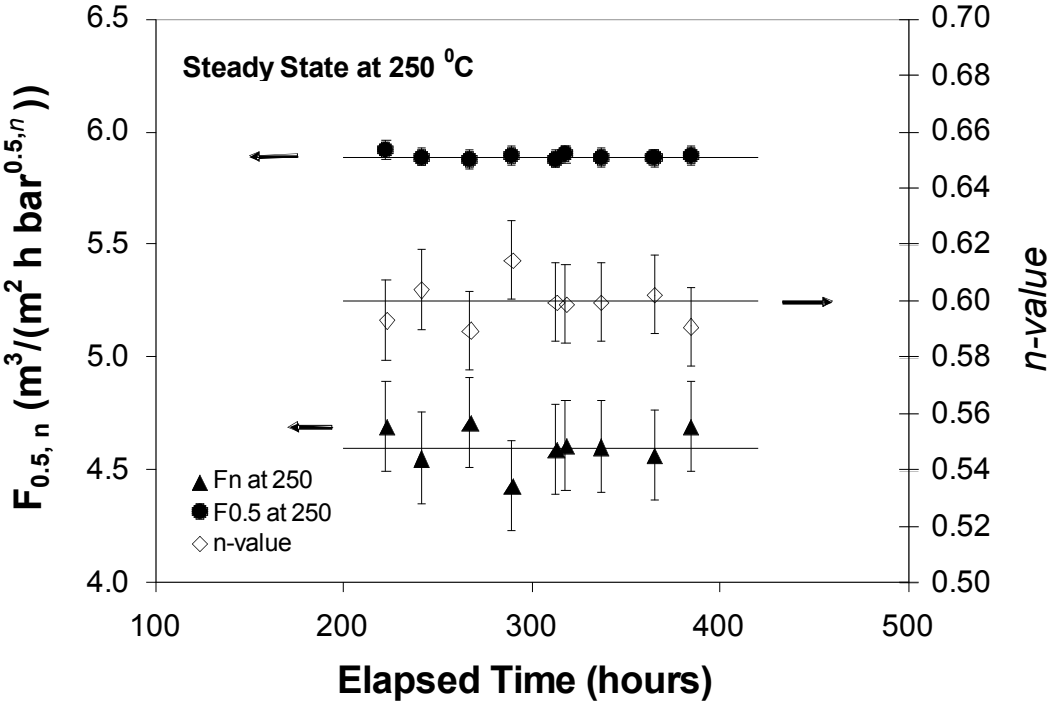

Figure A.1 $F_{0.5}$, F_n and n-exponent at 250ºC of membrane C01-F05. Ten measurements were used to compute standard deviations and estimate confidence intervals of $F_{0.5}$, F_n and n-exponent

Table A.1 Statistical analyses on permeance and n-exponent at 250ºC, membrane C01-F05

	n-exponent	H_2 Permeance ($m^3/(m^2\ h\ bar^n)$)	H_2 Permeance (n=0.5) ($m^3/(m^2\ h\ bar^{0.5})$)
Average	0.60	4.60	5.89
Calculated standard dev.	0.007	0.09	0.02
Considered standard dev.	0.014	0.2	0.04
Confidence interval (99%)	0.014	0.2	0.04

The high precision in data collection was achieved in this work by using digital mass flow meters, pressure transducers and continuously logging data.

The standard deviation of the H_2 permeance determined from a non-linear fit was 0.09 $m^3/(m^2\ h\ bar^{0.6})$, which was slightly larger than the permeance determined by assuming the Sieverts' law. Indeed, even though the non-linear fit of the experimental data was better than the linear fit (assuming *n* equal to 0.5), the nature of the mathematical expression involved in the fitting procedure (an exponential function of *n*) rendered the calculated H_2 permeance very sensitive to the n-exponent. The standard deviation of the n-exponent, also listed in Table A.1, was found to be equal to 0.007. Figure A.1 clearly shows the high standard deviation of F_n and the n-exponent resulting from the calculated H_2 permeance being extremely sensitive to the n-exponent fitting parameter. Moreover, the standard deviation calculated from any data set containing ten measurements could be as far as 60% from the real standard deviation. More than 100 measurements would be needed to determine a more accurate standard deviation, yet the time needed to collect such an enormous amount of data was prohibitive in this case. Therefore, the actual standard deviation of H_2 permeance determined assuming the Sieverts' law could be as high as 0.04 $m^3/(m^2\ h\ bar^{0.5})$ and as high as 0.014 for the n-exponent. Considering 0.014 as the

standard deviation of the n-exponent, the standard deviation of F_n was calculated to be 0.2 $m^3/(m^2\ h\ bar^{0.5})$. Calculated standard deviations, adjusted standard deviations due to insufficient number of measurements and confidence intervals are given in Table A.1 and were assumed to be the same at all temperatures.